

New Ctenodactyloid Rodents from the Erlian Basin, Nei Mongol, China, and the Phylogenetic Relationships of Eocene Asian Ctenodactyloids

Authors: Li, Qian, and Meng, Jin

Source: American Museum Novitates, 2015(3828) : 1-20

Published By: American Museum of Natural History

URL: <https://doi.org/10.1206/3828.1>

BioOne Complete (complete.BioOne.org) is a full-text database of 200 subscribed and open-access titles in the biological, ecological, and environmental sciences published by nonprofit societies, associations, museums, institutions, and presses.

Your use of this PDF, the BioOne Complete website, and all posted and associated content indicates your acceptance of BioOne's Terms of Use, available at www.bioone.org/terms-of-use.

Usage of BioOne Complete content is strictly limited to personal, educational, and non - commercial use. Commercial inquiries or rights and permissions requests should be directed to the individual publisher as copyright holder.

BioOne sees sustainable scholarly publishing as an inherently collaborative enterprise connecting authors, nonprofit publishers, academic institutions, research libraries, and research funders in the common goal of maximizing access to critical research.

New ctenodactyloid rodents from the Erlian Basin, Nei Mongol, China, and the phylogenetic relationships of Eocene Asian ctenodactyloids

QIAN LI,^{1, 2} AND JIN MENG^{1, 3}

ABSTRACT

During the last decade, numerous ctenodactyloid rodent fossils have been systematically collected from at least six horizons of the strata that are distributed from the upper part of the Nomogen Formation to the lower part of the Irдин Manha Formation in the Huheboerhe-Nuhetingboerhe area of the Erlian Basin, Nei Mongol (Inner Mongolia). The ages of these fossiliferous horizons range from the Earliest Eocene to the Middle Eocene. These fossils represent the best-known ctenodactyloid assemblages with a high species diversity and reliable stratigraphic and chronological constraints from one locality in central Asia. The fossils show a relatively continuous record of ctenodactyloids and the earliest radiation of rodents in central Asia beginning from the earliest Eocene. These data are important for biostratigraphic correlation of the Paleogene in central Asia and for understanding the taxonomy of Asian ctenodactyloids and the earliest diversity and evolution of rodents. Among the new fossils, we recognized 10 species that belong to six genera and three morphotypes. Of these taxa, three new genera and species, *Chenomys orientalis*, gen. et sp. nov., *Simplicimys bellus*, gen. et sp. nov., and *Yongshengomys extensus*, gen. et sp. nov., are described. In addition, three new species of *Tamquammys*, *T. robustus*, sp. nov., *T. longus*, sp. nov., and *T. fractus*, sp. nov., and one new species of *Yuomys*, *Y. huheboerhensis*, sp. nov., are also named. With these new materials, we are able to briefly review some existing problems in the taxonomy of early ctenodactyloids, which has

¹ Key Laboratory of Vertebrate Evolution and Human Origins of Chinese Academy of Sciences, Institute of Vertebrate Paleontology and Paleoanthropology, Chinese Academy of Sciences, Beijing.

² State Key Laboratory of Palaeobiology and Stratigraphy, Nanjing Institute of Geology and Palaeontology, Chinese Academy of Sciences, Nanjing.

³ Division of Paleontology, American Museum of Natural History, New York.

remained a difficult task in the study of this Asian rodent group. In light of the new material and taxonomic review, we conducted phylogenetic analyses of ctenodactyloids using a data matrix that contains 38 taxa and 81 characters. Our analysis shows that *Chenomys*, *Tamquammys*, and *Simplicimys* are placed at the base of the clade that contains the extant *Ctenodactylus*. *Yongshengomys* is the only taxon that is deeply placed within the clade containing the extant *Ctenodactylus* and clustered with *Chuankueimys* and *Tsinlingomys*. Our analysis supports Gobiomyidae and Ctenodactylidae as monophyletic groups, respectively, but shows that other families and subfamilies traditionally recognized, such as Cocomyinae, Advenimurinae, Tamquammyidae, Yuomyidae, and Chapattimyidae, are probably paraphyletic.

INTRODUCTION

The earliest known radiation of rodents of modern aspect in Asia took place during the earliest Eocene, represented by several ctenodactyloid rodents known primarily from China (Li et al., 1979, 1989; Dawson et al., 1984; Tong and Dawson, 1995; Tong, 1997; Meng and Li, 2010) and Mongolia (Shevyreva, 1989; Dashzeveg, 1990a, 1990b). Diverse ctenodactyloid rodents had a temporal distribution from the lower Eocene to lower Miocene of eastern and central Asia (Flynn et al., 1986). This group of rodents was ecologically well adapted in the region and had been one of the dominant rodent groups during most period of the Cenozoic. Because of their high diversity, rapid evolution of morphology and rich fossil records, ctenodactyloids have been an important group of mammals for biostratigraphic division and correlation, particularly in the Paleogene of Asia (Tong, 1997; Qiu and Qiu, 1995; Wang, 1997).

Basal ctenodactyloid rodents, as the earliest and one of most primitive rodents, have played a key role in many phylogenetic analyses that focused on Glires (Meng et al., 2003; Asher et al., 2005), Paleogene rodents (Marivaux et al., 2004), or hystricognathous rodents (Marivaux et al., 2002). However, because many Paleogene ctenodactyloids were based on fragmentary specimens and were often poorly presented in previous studies so that their morphologies have not been sufficient and clear enough to stabilize their taxonomies. For instance, several taxa from the early Eocene Bumban beds of Mongolia were established on fragmentary jaws and isolated teeth (Dashzeveg, 1990a, 1990b), but because the poor preservation and/or presentation of those specimens in the literature, others have considered some of the Bumban species to be either inadequately known (Tong and Dawson, 1995) or taxonomically invalid (Averianov, 1996). Hartenberger (in Meng and Li, 2010) raised similar concerns about validity of some Bumban ctenodactyloid rodents. The uncertainty in taxonomy of early ctenodactyloid rodents makes it difficult for anyone to engage in meaningful phylogenetic analyses that involve these Paleogene forms. To clarify at least some of these taxonomic problems, a thorough investigation of the existing specimens is required. For that purpose it will be helpful to have additional and better materials that provide more evidence on morphology of ctenodactyloid rodents and species variation and diversity. It is also crucial to have better chronological constraints on these rodent assemblages when we consider their taxonomic and phylogenetic relationships and interpret their evolution patterns.

A considerable collection of rodent specimens from the Huheboerhe-Nuhetingboerhe area of the Erlian Basin, Nei Mongol (Inner Mongolia), China, has been made over about 10 field seasons during the last decade. Previous studies already reported several rodents represented by a few specimens from the same area (Dawson, 1964; Qi, 1987). The rodent specimens reported here were collected by surface

prospecting and screen-washing from several localities in the area where stratigraphic data were systematically recorded. These new specimens have significantly expanded the composition of mammal faunas, particularly the microfaunas, from this region. In this study we will document exclusively the new material of ctenodactyloid rodents from six horizons ranging from the lowest Eocene to the middle Eocene of the area. Other groups of rodents and mammals will be treated in separate researches. The ctenodactyloid rodents in collections are represented by partial skulls, fragmentary maxillae, mandibles, and numerous isolated teeth; they provide a considerable amount of new morphology and diversity. Our work will focus on the description of the new specimens and their taxonomic assignment based primarily on dental morphologies. In light of the new data, we are able to conduct phylogenetic analyses and provide new insight into some existing issues in the taxonomy and phylogeny of the Eocene ctenodactyloids. However, given the limited material of many previously known species and our lack of access to most type specimens of the species reported in previous studies, in which the specimens were poorly illustrated, we found it still difficult, thus beyond the scope of this study, to conduct a systematic review and to resolve many taxonomic and phylogenetic problems of Eocene ctenodactyloids in Asia. Nonetheless, the new data reported here add new information on the temporal and geographic distributions of the earliest to middle Eocene rodents of Asia. With reasonable constraints on the superposition of stratigraphic and magnetostratigraphic data of the rock sequences where the fossils were collected, these rodent assemblages furnish one of the best-known references for biostratigraphic correlations in the Eocene of central Asia. The diverse species from the six horizons will undoubtedly help us to understand the early radiation and evolution of this Paleogene rodent group of Asia.

MATERIALS AND METHODS

For the taxonomy of ctenodactyloids, we only use Ctenodactyloidea as the superfamily level taxon, because the family-level classification of early ctenodactyloids remains unstable. All specimens reported in this study were collected from the Huheboerhe-Nuhetingboerhe area. Stratigraphic horizon and GPS coordinates were recorded to document the specific site where each specimen was collected. In describing the specimens we use the dental terminology illustrated in figure 1, which is modified from Wang (1997), Tong (1997), and Meng and Wyss (2001). Measurements of teeth were taken using an Olympus SZX7 microscope with an accuracy of 0.01 mm. SEM photographs of uncoated teeth were taken using a JSM-6100 SEM machine at the Institute of Vertebrate Paleontology and Paleoanthropology, Beijing.

Institutional abbreviations: AMNH, American Museum of Natural History, New York; IVPP, Institute of Vertebrate Paleontology and Paleoanthropology, Beijing, where all the specimens were deposited.

GEOLOGICAL SETTING

The Erlian Basin is located in central Nei Mongol, close to the border with Mongolia. The Cenozoic beds in the basin were first explored by the Central Asiatic Expeditions (CAE) of the American Museum of Natural History in the 1920s (Granger and Berkey, 1922; Berkey and Granger, 1923; Berkey and Morris, 1924, 1927; Matthew and Granger, 1926). Since the investigations of the CAE, a number of fossil mammal localities spanning an interval from the Late Paleocene to the Oligocene have been discovered

and have produced many mammal specimens (Russell and Zhai, 1987). However, because the regional stratigraphic and locality data have been imprecise since the work of the CAE (Radinsky, 1964), considerable efforts were made to clarify the lithological and biostratigraphic correlations and localities among several key sections in the area (Meng, 1990; Meng et al., 2004, 2007b; Bowen et al., 2005; Wang et al., 2010, 2012). The Huheboerhe-Nuhetingboerhe area includes the escarpment through which several sections have been measured, including the Huheboerhe, Nuhetingboerhe, Daoteyin Obo, and Wulanboerhe sections (Meng et al., 2007b; Wang et al., 2012). The rock sequence in the area comprises three lithological units, the Nomogen, Arshanto and Irдин Manha formations, with a total thickness of 82.4 m (Meng et al., 2007b). Twelve mammal-bearing horizons have been recognized in the sequence, including four in the Nomogen Formation, six in the Arshanto Formation, and two in the Irдин Manha Formation. These horizons are denoted as, in ascending order, NM-1 to NM-4 (for the Nomogen Formation), AS-1 to AS-6 (Arshanto Formation), and IM-1 to IM-2 (Irдин Manha Formation) (Wang et al., 2010). The paleomagnetic study (Sun et al., 2009) suggests that the upper part of the Nomogen Formation is the lowest Eocene and the Arshanto Formation is mainly the upper part of the Lower Eocene rather than the lower part of the Middle Eocene; the latter was the conventional view of the age of the Arshanto Formation (Li and Ting, 1983; Russell and Zhai, 1987). The up-to-date locality map can be found in Wang et al. (2012: fig. 1).

The ctenodactyloid specimens described here were collected from the upper part of the Nomogen Formation (NM-3), several horizons of the Arshanto Formation (AS-1, AS-2, AS-3, and AS-5) and the lower Irдин Manha Formation (IM-1) in the Huheboerhe-Nuhetingboerhe area (fig. 2). Various mammals collected during the past few years, including rodents and lagomorphs (Li et al., 2007), perissodactyls (Bai et al., 2010), primates (Ni et al., 2007, 2009), basal Glires (Meng et al., 2004; 2007a, 2007c; 2009), mesonychids (Jin, 2012), and coryphodontids (Mao and Wang, 2012), have been reported from these horizons. Rodents known from the Huheboerhe-Nuhetingboerhe area included the ctenodactyloid *Yuanomys* from NM-3 (Meng and Li, 2010), *Archetypomys* (Meng et al., 2007a) and a primitive myodont *Erlanomys* from AS-1 (Li and Meng, 2010), some cricetids (*Pappocricetodon neimongolensis*, *Pappocricetodon* sp., *Pappocricetodon* cf. *P. zhongtiaensis*) from IM-1 (Li, 2012), the ischyromyid *Asiomys dawsoni* from IM-1, and a generically indeterminate ischyromyid from AS-1 (Li and Meng, 2013).

SYSTEMATIC PALEONTOLOGY

Rodentia Bowdich, 1821

Ctenodactyloidea Simpson, 1945

Tamquammys wilsoni Dawson et al., 1984

HOLOTYPE: IVPP V5678, an anterior portion of skull with broken incisors, right P4, left DP3–M3 (Dawson et al., 1984).

PARATYPES: V5679–5683, mandibles and molars, Camp Margetts area, Nei Mongol (for locality names, see Meng et al., 2007b; Wang et al., 2010, 2012).

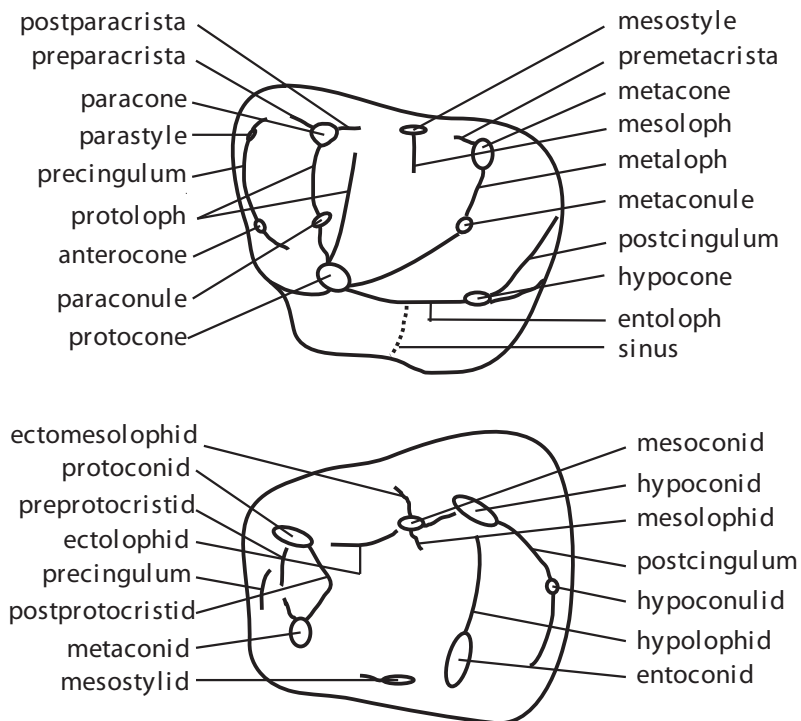


FIG. 1. Diagram showing the terminology applied to ctenodactyloid dental morphology (anterior to the left and labial to the top) (modified from Wang, 1997; Tong, 1997; Meng and Wyss, 2001).

REFERRED SPECIMENS: Referred specimens were collected from several horizons and are listed from the lowest to the highest level in the stratigraphic sequence (see fig. 2 for reference). **NM-3:** V16886, left M2. **AS-1:** V17793.1–80, left P3; V17793.81–159, right P3; V17793.160–178, left DP4; V17793.179–196, right DP4; V17793.197–255, left P4; V17793.256–304, right P4; V17793.305–411, left M1; V17793.412–497, right M1; V17793.498–599, left M2; V17793.600–693, right M2; V17793.694–758, left M3; V17793.759–829, right M3; V17794.1–16, left dp4; V17794.17–36, right dp4; V17794.37–66, left p4; V17794.67–106, right p4; V17794.107–172, left m1; V17794.173–241, right m1; V17794.242–347, left m2; V17794.348–441, right m2; V17794.442–520, left m3; V17794.521–596, right m3; V17795, right mandible with p4–m3; V17796, left mandible with p4–m3. **AS-2:** V17784, left maxilla with M1–3; V17785.1, right maxilla with P3–M2; V17785.2, left maxilla with P3–M1; V17786.1–2, right mandibles with p4–m3; V17786.3, left mandible with p4–m2; V17786.4, left mandible with m1–3; V17786.5–10, left mandibles with m1–2; V17786.11, left mandible with m2; V17786.12, right mandible with p4–m3; V17786.13–17, right mandibles with m1–2; V17786.18–19, right mandibles with m1–3; V17786.20, right mandible with m2–3; V17787.1, left mandible with dp4–m2; V17787.2–5, right mandibles with dp4–m2; V17788.1–2, right P4; V17788.3, left M1; V17788.4–6, right M1; V17788.7, left M2; V17788.8–9, right M2; V17788.10, right M3; V17789, right m3; V17790, right maxilla with P3–M3; V17791.1, left mandible with m2; V17791.2–3, left mandibles with m1–2; V17791.4, right mandible with m1–2; V17791.5, right mandible with m1–2 and erupting p4; V17791.6, right mandible with m1–3; V17791.7, left mandible

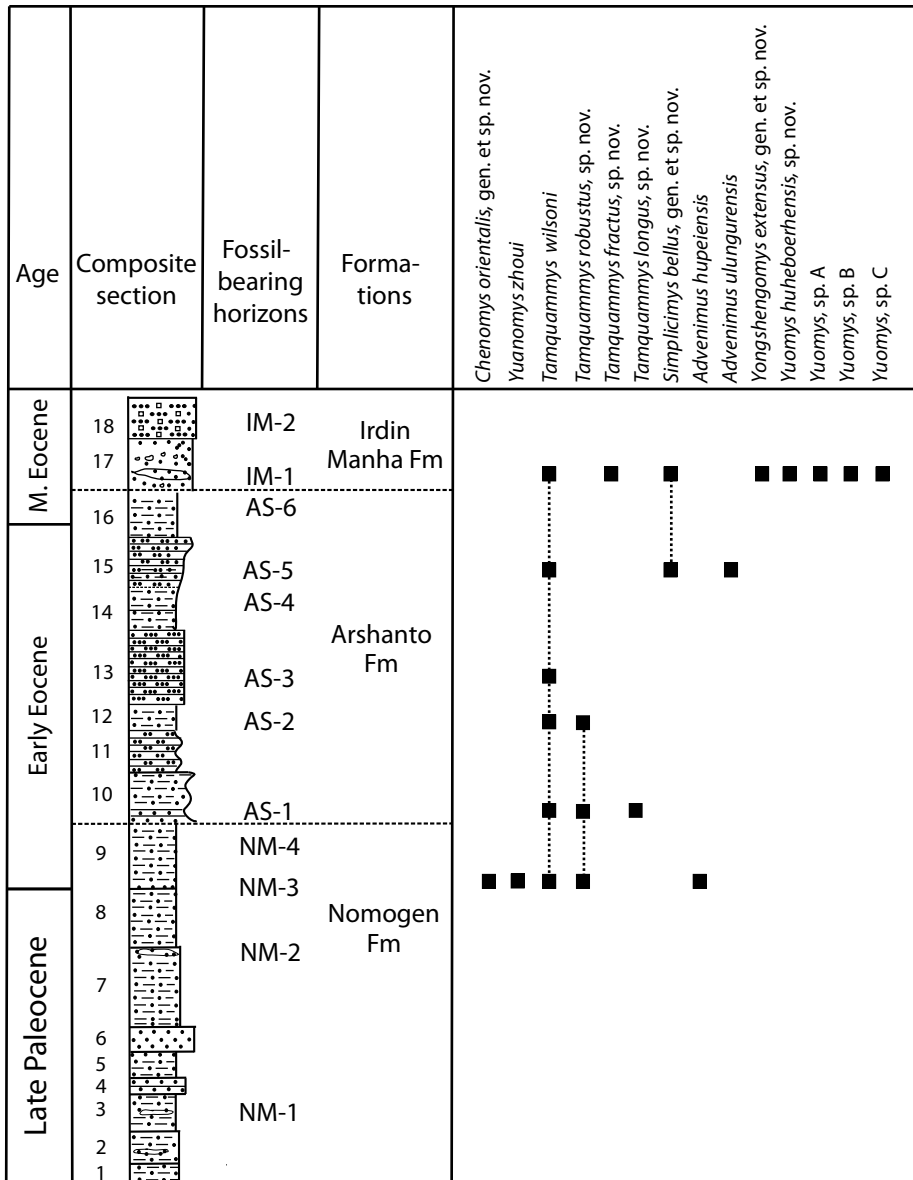


FIG. 2. Stratigraphic distribution of ctenodactyloid taxa in the Huheboerhe-Nuhetingboerhe area, plotted on a composite section modified from Wang et al. (2010). Fossil horizons are denoted as, in ascending order, NM-1 to NM-4 in the Nomogen Formation, AS-1 to AS-6 in the Arshanto Formation, and IM-1 to IM-2 in the Irdin Manha Formation (modified from Wang et al., 2010: fig. 2). Black squares indicate occurrences of ctenodactyloid species from the fossil horizons that were described in this study.

with m1–2; V17791.8–10, left mandibles, each with m1–2; V17791.11, right mandible p4–m2; V17791.12, right mandible with m1; V17791.13–14, right mandibles with m1–2; V17791.15–16, right mandibles with m3; V17792, juvenile maxilla with DP4–M1. **AS-3:** V17806.1, right mandible with p4–m3; V17806.2, right mandible with m1–2; V17807.1, right DP4; V17807.2–3, left P4; V17807.4–6, left M1;

V17807.7–11, right M1; V17807.12–15, left M2; V17807.16, right M2; V17807.17–18, right M3; V17808.1, left dp4; V17808.2–6, left m1; V17808.7–8, right m1; V17808.9–10, right m2; V17808.11, left m3. **AS-5:** V17809.1–2, left P4; V17809.3, right P4; V17809.4–8, left M1; V17809.9–12, right M2; V17810.1, right p4; V17810.2–7, left m1; V17810.8–11, right m1; V17810.12–21, left m2; V17810.22–33, right m2; V17810.34–37, left m3; V17810.38–42, right m3. **IM-1:** V17811.1–3, left P4; V17811.4–7, right P4; V17811.8–15, left M1; V17811.16–24, right M1; V17811.25–32, left M2; V17811.33–38, right M2; V17811.39–43, left M3; V17811.44–47, right M3; V17812.1–3, left p4; V17812.4–8, right p4; V17812.9–10, left m1; V17812.11–14, right m1; V17812.15–25, left m2; V17812.26–35, right m2; V17812.36–43, left m3; V17812.44–52, right m3.

LOCALITY AND HORIZON: Huheboerhe-Nuhetingboerhe area, Erlian Basin, Nei Mongol; NM-3, AS-1, AS-2, AS-3, AS-5, and IM-1; Early–Middle Eocene (fig. 2).

EMENDED DIAGNOSIS: Small ctenodactyloid; cheek teeth brachydont and increase in size distally; P4 and p4 nonmolariform; the protoloph and metaloph complete on P4, protocone connected to paracone; each upper molar with two protolophs, distinct paraconule and metaconule, and a weak connection between metaconule and protocone; sinus between the protocone and hypocone shallow; the masseteric crest extending anteriorly to below m2; p4 with isolated protoconid and metaconid, but without hypoconulid; the preprotocristid and postprotocristid of lower molars well developed; the hypoconulid and mesoconid of lower molars distinct; the ectolophid complete; the hypolophid of m1 extending to the hypoconulid; the hypolophid on m2 and m3 transverse and extending to the hypoconid or ectolophid.

DESCRIPTION

Among the specimens referred to *Tamquammys wilsoni* there are two maxillae that come from juvenile or young individuals because they contain deciduous teeth (fig. 3B). Each maxilla bears a partial zygomatic process that begins anteriorly at the level of DP3 and terminates posteriorly above DP4. In ventral view of the maxilla, the posterior edge of the incisive foramen is situated close to the anterior part of DP3, more anteriorly placed than in *T. dispinorum* and *T. tantillus*.

The partial lower jaws are of typical sciurognathous form. The body of the mandible is slender, and the horizontal ramus is flat ventrally. The ascending ramus is not preserved in specimens of our collection. From 20 specimens, the height of mandible varies from 3 to 3.5 mm, measured at m1. On the lateral surface of the mandible the masseteric fossa is deep and extends anteriorly to below m2. There are two mental foramina, a large one located below the anterior part of p4 and a small one below p4. The diastema measures 2–2.5 mm in length. The lower incisor is slender, oval in cross section, and, as revealed by breakage of the jawbone, extends posteriorly farther than m3.

P3 is small, peglike and single rooted, with an oval outline in occlusal view. The main cusp of P3 is high and conical, with a distinct cingulum on its labial side (figs. 3A, 4J–K; table 1).

DP4 has a molariform tooth pattern with subequal paracone and metacone on the labial side, and a well-developed protocone, and a small hypocone on the lingual side (figs. 3B, 4H–I). The hypocone is a lingually positioned, poorly developed cusp on the postcingulum. The paraconule is small and anterolingual to the paracone. The metaconule is distinct and larger than the paraconule. The mesostyle is weak or absent. The precingulum is distinct and meets a small parastyle at the anterolabial corner of the tooth.

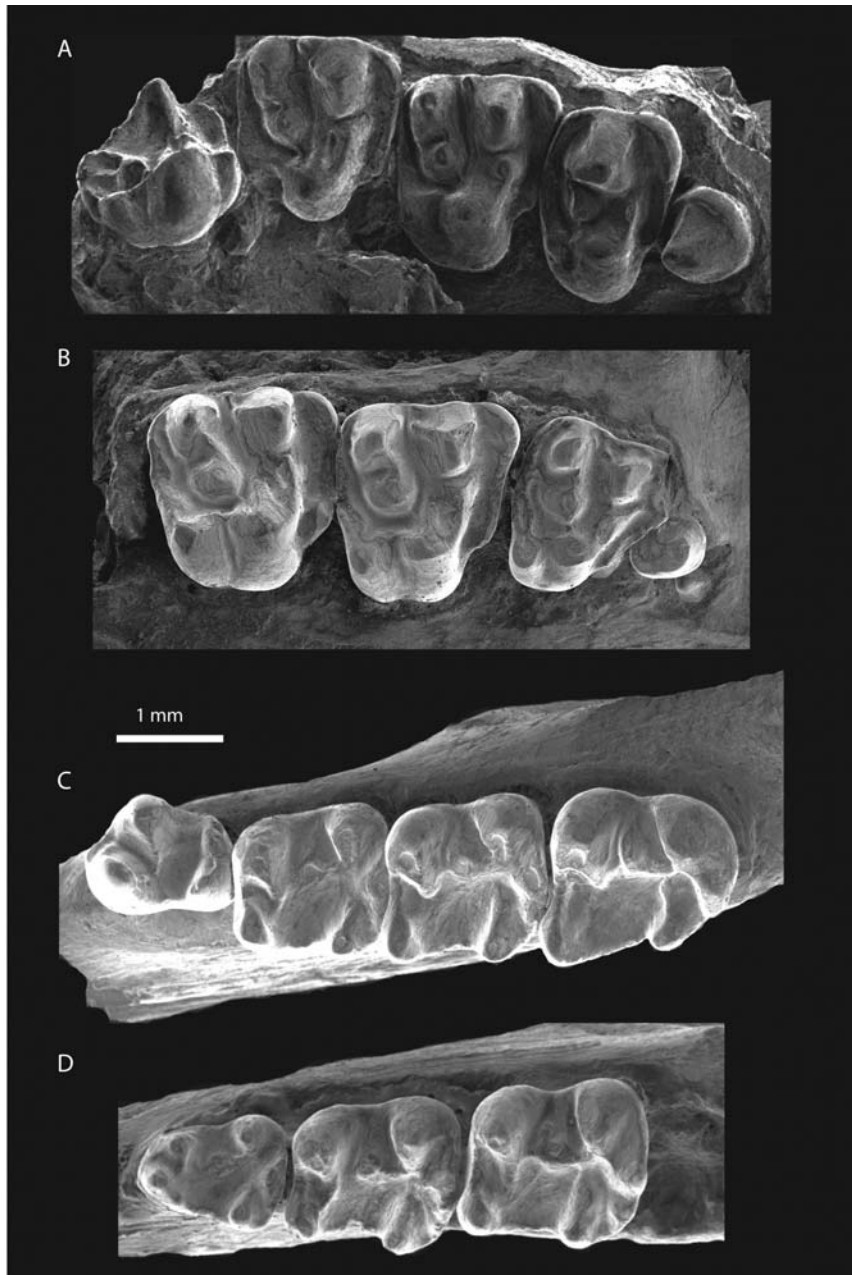


FIG. 3. Fragmentary maxillae and mandibles of *Tamquammys wilsoni* in occlusal view. **A**, V17790, a right maxilla with P3–M3; **B**, V17785.1, a right maxilla with P3–M2; **C**, V17786.2, a right mandible with p4–m3; **D**, V17787.5, a right mandible with dp4–m2.

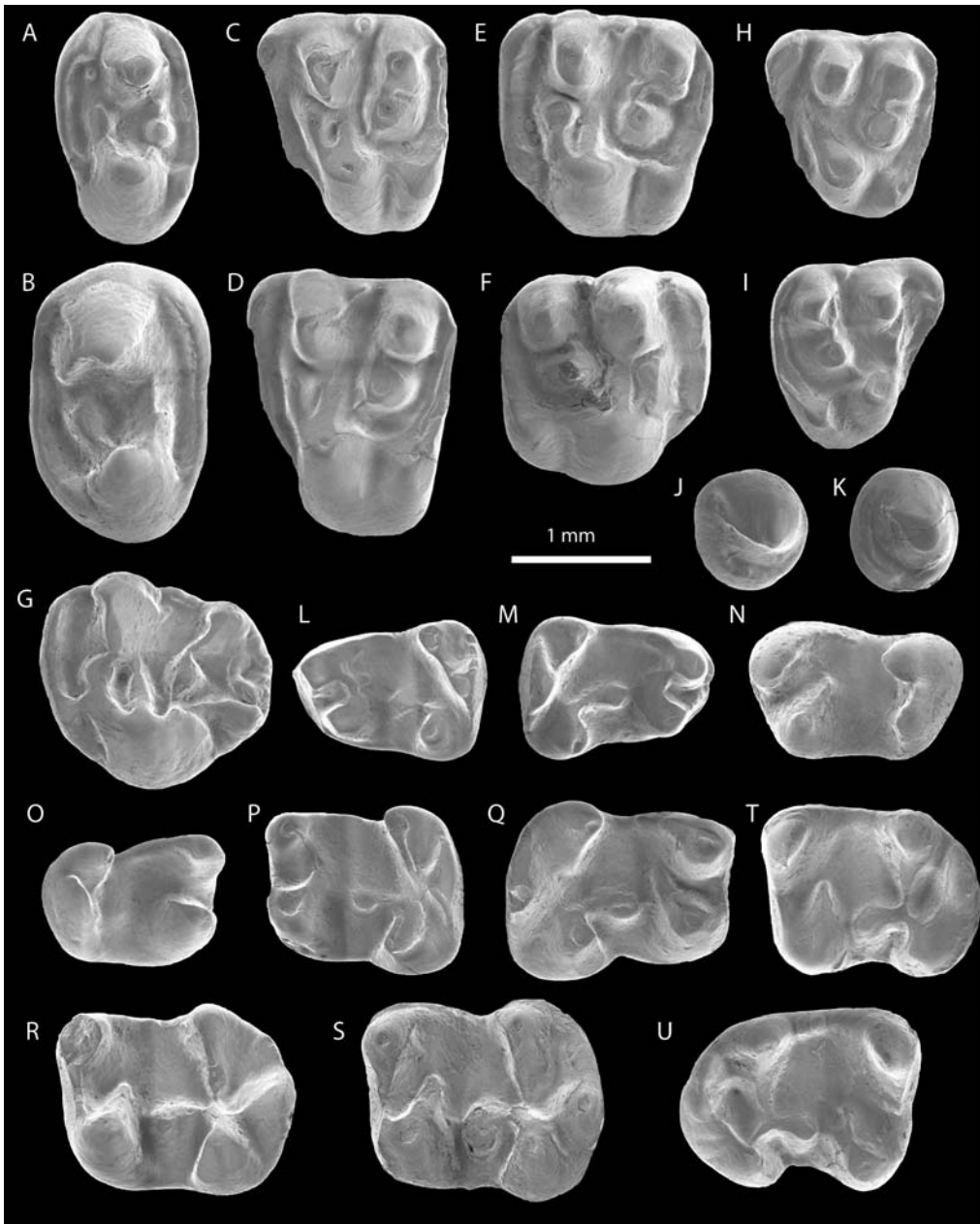


FIG. 4. Cheek teeth of *Tamquammys wilsoni* in occlusal view. **A**, V17793.201, left P4; **B**, V17793.303, right P4; **C–D**, V17793.307, V17793.369, left M1; **E**, V17793.556, left M2; **F**, V17793.663, right M2; **G**, V17793.696, left M3; **H**, V17793.172, left DP4; **I**, V17793.180, right DP4; **J–K**, V17793.9, V17793.80, left P3; **L**, V17794.4, left dp4; **M**, V17794.36, right dp4; **N**, V17794.37, left p4; **O**, V17794.69, right p4; **P**, V17794.128, left m1; **Q**, V17794.179, right m1; **R–S**, V17794.245, V17794.292, left m2; **T**, V17794.458, left m3; **U**, V17794.538, right m3.

TABLE 1. Measurements of the cheek teeth in various species of *Tamquammys* (mm).

Name	<i>T. wilsoni</i>		<i>T. wilsoni</i>		<i>T. robustus</i>		<i>T. robustus</i>		<i>T. longus</i>		<i>T. fractus</i>	<i>T. dispinorum</i>		<i>T. tantillus</i>	
Horizon	AS-1	AS-2	AS-1	AS-2	AS-1	AS-2	AS-1	AS-2	AS-1	AS-2	IM-1	Hetaoyuan Formation	Zaisan Basin		
	Min-max	Mean	Min-max	Mean	Min-max	Mean	Min-max	Mean	Min-max	Mean		Min-max	Mean		
P3	L	0.53-0.9	0.77	0.4	0.4	0.82-1.39	1.07	0.8	0.8	—	—	—	0.6	0.6	0.99
	W	0.52-1.05	0.84	0.25	0.25	0.95-1.62	1.19	0.72	0.72	—	—	—	0.7	0.7	1.05
DP4	L	1.03-1.51	1.32	1.2-1.6	1.43	1.41-1.97	1.56	1.52-1.68	1.59	1.5	1.5	—	1.3	1.3	—
	W	1.04-1.83	1.51	1.5-2	1.73	1.45-2.11	1.74	1.6-1.76	1.68	1.5-1.6	1.55	—	1.4	1.4	—
P4	L	0.96-1.39	1.19	1.4	1.4	1.41-1.82	1.56	1.6	1.6	—	—	—	0.9-1.3	1.11	1.45
	W	1-2.29	1.79	1.9	1.9	2.12-2.67	2.37	2.8	2.8	—	—	2.25	1.5-1.9	1.68	1.75
M1	L	1.17-1.69	1.45	1.3-1.65	1.48	1.73-2.21	1.93	1.92-2.16	2	1.8	1.8	1.7	1.2-1.4	1.36	—
	W	1.36-2.02	1.7	1.6-2	1.76	1.84-2.48	2.14	2-2.4	2.28	2.1	2.1	2.2	1.4-1.8	1.65	—
M2	L	1.29-1.75	1.52	1.5-1.8	1.59	1.83-2.45	2.15	2-2.4	2.25	1.9-2	1.95	1.8	1.3-1.7	1.51	—
	W	1.42-1.96	1.69	1.65-1.8	1.71	1.94-2.65	2.32	2.24-2.56	2.46	2.3	2.3	2.2	1.4-1.75	1.57	—
M3	L	1.38-1.89	1.64	1.4-1.7	1.53	2.16-2.78	2.48	2.48-2.64	2.58	2.1-2.15	2.13	—	1.5-1.65	1.55	—
	W	1.18-1.72	1.49	1.4-1.7	1.51	1.81-2.53	2.2	2.4	2.4	2.1	2.1	—	1.3-1.6	1.51	—
dp4	L	1.26-1.52	1.42	1.28-1.48	1.38	1.52-1.78	1.62	1.36-1.6	1.48	—	—	—	—	—	—
	W	0.9-1.19	1.04	0.96-1.12	1.04	1.04-1.6	1.18	1.28-1.36	1.32	—	—	—	—	—	—
p4	L	1.22-1.59	1.41	1.1-1.44	1.29	1.64-2.26	1.91	1.6-2	1.74	—	—	—	1.2-1.4	1.3	—
	W	0.88-1.17	1.03	0.8-1	0.96	1.29-1.65	1.42	1.44-1.52	1.48	—	—	—	1-1.2	1.11	—
m1	L	1.4-1.78	1.61	1.36-1.68	1.53	1.81-2.29	2.09	1.92-2.4	2.1	—	—	—	1.5-1.65	1.57	—
	W	1.13-1.6	1.32	1.2-1.68	1.45	1.4-1.9	1.69	1.5-2.08	1.77	—	—	—	1.15-1.3	1.21	—
m2	L	1.38-2	1.71	1.3-1.8	1.65	1.97-2.8	2.33	2-2.56	2.34	—	—	—	1.6-1.7	1.63	—
	W	1.08-1.72	1.42	1.28-1.7	1.45	1.69-2.3	1.99	1.76-2.4	2.15	—	—	—	1.3-1.4	1.34	—
m3	L	1.54-2.11	1.81	1.28-2	1.76	2.17-3.12	2.61	2.56-2.8	2.67	—	—	—	1.6-1.9	1.78	—
	W	1.11-1.68	1.4	1.2-1.6	1.4	1.65-2.45	1.99	2-2.4	2.16	—	—	—	1.3-1.5	1.4	—

The protoloph is complete and extends labially to contact the paracone. The metaloph connects the metacone to the metaconule and extends lingually to the base of the protocone.

P4 is nonmolariform and double rooted. This tooth is anteroposteriorly shorter than transversely wide and has a well-developed precingulum and postcingulum. The P4 crown has two main cusps, presumably homologous to the protocone lingual and to the paracone labially (figs. 3A, 4A–B). The protocone and paracone are subequal in size. Posterior to the protocone is a small but distinct hypocone, from which extends labially a complete postcingulum. A distinct conule posterolabial to the protocone is identified as the metaconule. A complete protoloph connects the protocone to the paracone. The metaconule is connected to the protocone by a low metaloph, which usually joins the lingual side of the protocone (fig. 4B), but in some specimens it is too weakly developed to reach the protocone (fig. 4A).

M1 is quadrate in crown outline and triple rooted, having two small labial roots and one major lingual one. It is low crowned and has distinct cusps and conules (figs. 3A–B, 4C–D). The protocone, paracone, and metacone are all well developed. A distinct hypocone is present but smaller than the protocone; it gives the tooth an approximately square appearance in lingual occlusal view. The metaconule is large, subequal in size to the metacone. The protocone has two strong parallel protoloph (present in 180 specimens of a total of 195 specimens): the anterior one usually ends at the paraconule anterolingual to the paracone but in some specimens extends to the paracone; the posterior one extends labially to the base of the paracone at the lingual. In the rest specimens (15 of 195), the protocone is connected to the paracone by a single complete protoloph. A weak metaloph extends from the metacone to the metaconule, whereas the metaconule and protocone may be either isolated or connected by a weak loph. The entoloph joins the protocone to the hypocone, forming the edge of the lingual valley. The sinus is shallow. The mesostyle is small. The precingulum is well developed, with its lingual end expanded to form a cusp and its labial end reaching a distinct parastyle on the anterolabial corner of the tooth.

M2 is similar to M1 in its general morphology, but is larger. The cusps are more prominent than those of M1, and the protolophs are more distinct (fig. 4E–F).

M3 has a rounded triangular outline in occlusal view (figs. 3A, 4G). The metacone is reduced, and the hypocone is slightly labially displaced and smaller than those in M1 and M2. The paraconule and metaconule are well developed. The anterior and posterior protoloph are complete, reaching the paracone.

The dp4 is molariform and mesiodistally long. Its trigonid is narrower than the talonid (figs. 3D, 4L–M). The metaconid is close to the protoconid and is slightly anteriorly placed. A weak precingulum is present on the anterior side of the base of the crown in some teeth. The postprotocristid extends posterolingually to reach the metaconid and close the trigonid basin distally. The entoconid is distinct, with a short hypolophid extending to the hypoconulid. The hypoconid is either separated from the hypoconulid by a notch or connected to the latter by a weak ridge. The hypoconulid is conspicuously large and extends transversely along the posterior margin of the tooth. The ectolophid is low and straight, with a distinct mesoconid at its middle point.

The p4 differs from dp4 in being shorter and nonmolariform. The trigonid of the tooth is higher and slightly wider than the talonid and consists of two main cusps, presumably the metaconid and protoconid (fig. 3C). The metaconid is higher than the protoconid; they are usually separated from each other by a notch (fig. 4O), but in some teeth connected by a postprotocristid (fig. 4N). The talonid is simple, bearing only the entoconid and hypoconid; both cusps are lower than the protoconid and meta-

conid. The hypoconid is smaller than the entoconid. Neither a mesoconid nor a mesostylid is present, but a weak ectolophid is present in some specimens.

Each lower molar has two long roots, of which the posterior one is more robust. The lower cheek teeth increase in size distally (fig. 3C–D). The trigonid is significantly higher than the talonid. The metaconid is always higher than the protoconid in both juvenile and adult individuals.

The protoconid and metaconid of m1 are prominent and connected by a low but complete preprotocristid (fig. 4P–Q). The postprotocristid is well developed and extends to the base of the metaconid. The relatively low talonid has a conical entoconid and hypoconid, and a distinct hypoconulid that is situated at the midpoint of the posterior margin of the talonid. In most teeth (37 of 41) the hypolophid of m1 extends somewhat posterolabially from the entoconid to the hypoconulid, but occasionally it extends more transversely to the hypoconid (4 of 41). There is a low and complete ectolophid that bears a distinct mesoconid. No mesostylid is present.

The m2 is larger than m1. The m2 postprotocristid is distinct but weaker than that of m1. The hypolophid is variably developed. In most teeth it extends transversely and contacts the ectolophid in front of the hypoconid (27 of 38) (fig. 4R–S), or meets or closely approaches the hypoconid (7 of 38), but occasionally it contacts the hypoconulid (4 of 38).

On m3 the postcingulum-hypoconulid projects posteriorly, giving a rounded distal end of the tooth (fig. 4T–U). The transverse hypolophid contacts the ectolophid.

COMPARISONS

The new specimens from the Huheboerhe-Nuhetingboerhe area possess several typical tamquammyid features, including a sciurognathous lower jaw, cheek teeth increasing in size distally, well-developed conules in upper molars, distinct lophids in lower teeth, P4 nonmolariform with a labial cusp and a distinct metaconule, and p4 nonmolariform with the trigonid being slightly wider than the talonid.

Tamquammys is one of the first-described ancient ctenodactyloid genera, and includes three species: *T. tantillus*, *T. wilsoni*, and *T. dispinorum*. Shevyreva (1971) described *T. tantillus* from probable middle Eocene deposits of Zaisan Basin, Kazakhstan. *T. tantillus* is the type of *Tamquammys* (Shevyreva, 1971), but included only P4 and P3. *T. wilsoni* was based on specimens from the Arshanto Formation of Camp Margetts area, Nei Mongol (Dawson et al., 1984). *T. dispinorum* was from the Hetaoyuan Formation of Henan Province, China (Tong, 1997), based on a few fragments of the maxilla and mandible and some isolated cheek teeth. Wang et al. (2012) suggested that the Huheboerhe-Nuhetingboerhe area is roughly the same as the CAE's Camp Margetts area, so all known specimens of *T. wilsoni* probably came from the same bed of the area. The new specimens from the Huheboerhe-Nuhetingboerhe area resemble *T. wilsoni* in sharing several features, such as two parallel protolophs, a distinct paraconule on the anterior protoloph, an oblique hypolophid on m1, and a transverse hypolophid contacting the ectolophid or hypoconid on m2–3. In both *T. tantillus* and *T. dispinorum*, however, the paraconule on the anterior protoloph is reduced. In *T. tantillus* P4 lacks a metaconule. The p4 in *T. dispinorum* is more elongated than that of *T. wilsoni*, and the hypolophid on m1–2 contacts the hypoconid. Because of the similar features shared by the new specimens and the type specimens of *T. wilsoni* and because the specimens were collected from the same formation and area, we think it appropriate to assign the new specimens to *T. wilsoni*. Although the specimens assigned to the species display some variation in dental morpholo-

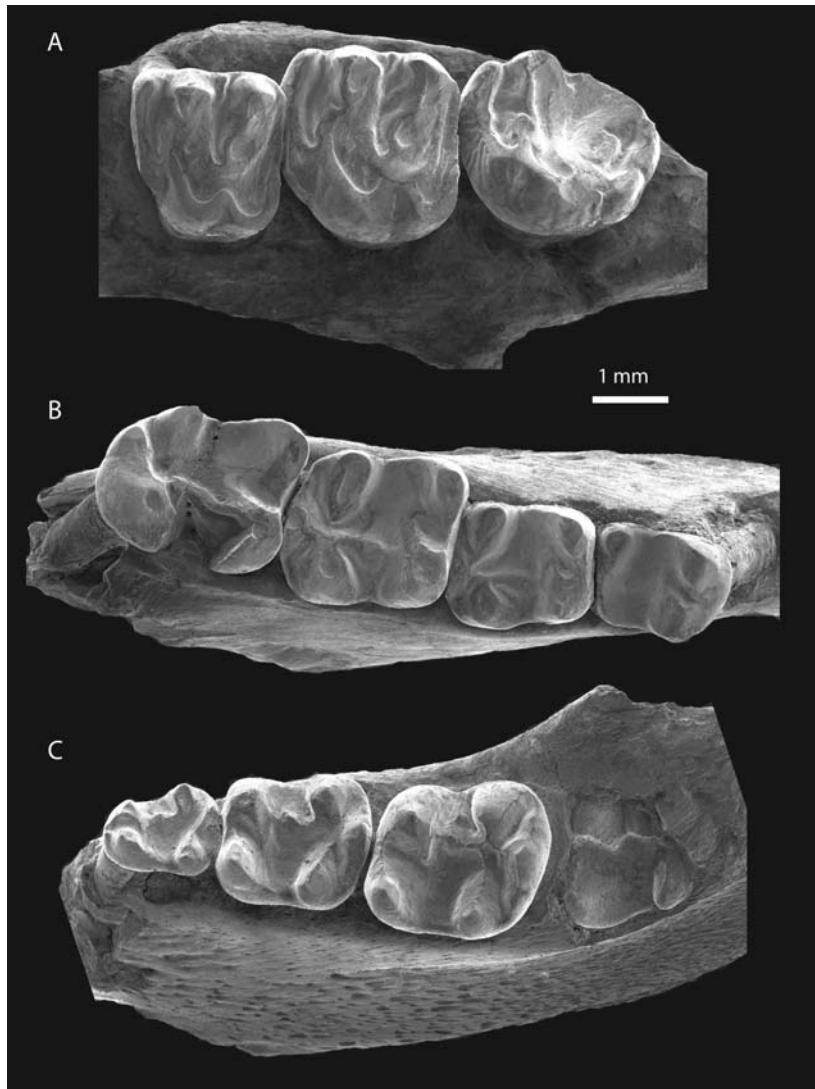


FIG. 5. Cheek teeth of *Tamquammys robustus*. **A**, V17770.1, an adult left maxillary fragment with M1–3; **B**, V17772.5, an adult right mandible fragment with p4–m3; **C**, V17773.5, a juvenile right mandible fragment with dp4–m3.

gies, there is sufficient evidence to place them into the same species and distinguish it from *T. tantillus*, *T. dispinorum*, and new species we name below.

Tamquammys robustus, new species

HOLOTYPE: V17770.1, left maxilla with M1–3 (fig. 5A) from AS-2 (fig. 2).

REFERRED SPECIMENS: **NM-3:** V16887, left M2. **AS-1:** V17777, partial skull with left broken M2 and right M2; V17778.1, partial skull with incisor and DP4–M2; V17778.2, partial skull with incisor and right DP4–M1; V17778.3, partial skull with left M1 and right M1, M3; V17779.1–27, left P3; V17779.28–

44, right P3; V17779.45–78, left DP4; V17779.79–117, right DP4; V17779.118–159, left P4; V17779.118–209, right P4; V17779.210–329, left M1; V17779.330–440, right M1; V17779.441–540, left M2; V17779.541–616, right M2; V17779.617–667, left M3; V17779.668–713, right M3; V17780.1–12, left dp4; V17780.13–29, right dp4; V17780.30–53, left p4; V17780.54–81, right p4; V17780.82–152, left m1; V17780.153–216, right m1; V17780.217–300, left m2; V17780.301–356, right m2; V17780.357–396, left m3; V17780.396–436, right m3; V17781.1, right mandible with p4–m1; V17781.2, right mandible with m1–2; V17782, right mandible with incisor and dp4–m2; V17783, right mandible with m1–2; V17797.1, left mandible with incisor, erupting p4 and m1–2; V17797.2, left mandible with incisor and m2; V17797.3, right mandible with incisor and m1. AS-2: V17770.2, left maxilla with P4–M2; V17771.1, partial skull with left DP4–M2; V17771.2, partial skull with left DP4–M1; V17771.3, left maxilla with DP3–M2; V17771.4–5, right maxillae with DP4–M1; V17772.1–3, left mandibles with m1–2; V17772.4, left mandible with m2; V17772.5, right mandible with incisor and p4–m3; V17772.6–7, right mandibles with m1–3; V17772.8–9, right mandibles with incisor and m1–2; V17772.10–11, right mandibles with m2; V17772.12, right mandible with erupting p4; V17773.1, left mandible with erupting p4 and m1–2; V17773.2, left mandible with m2 and erupting m3; V17773.3, left mandible with m1–2 and erupting m3; V17773.4, right mandible with dp4–m1; V17773.5, right mandible with dp4–m3; V17773.6, right mandible with incisor, erupting p4 and m1–2; V17774.1, left DP4; V17774.2, left M1; V17774.3–5, right M1; V17774.6–9, left M2; V17774.10–13, right M2; V17774.14, left M3; V17774.15–16, right M3; V17775.1, left p4; V17775.2–6, left m1; V17775.7–11, right m1; V17775.12–16, left m2; V17775.17, right m2; V17775.18, left m3; V17775.19, right m3; V17776.1, left mandible with m1; V17776.2, right mandible with broken m1 and m2; V17776.3, right mandible with incisor and broken m2.

LOCALITY AND HORIZON: Huheboerhe-Nuhetingboerhe area, Erlian Basin, Nei Mongol; NM-3, AS-1 and AS-2, Early Eocene (fig. 2).

DIAGNOSIS: The largest species of the genus with larger and more robust molar cusps and more distinct lophs than in *T. tantillus*, *T. wilsoni*, and *T. dispinorum* (table. 1). Further differs from *T. wilsoni* in having shorter postprotocristid on m1 and wider talonid of p4. Further differs from *T. tantillus* and *T. dispinorum* in having more oblique hypolophid on m1.

ETYMOLOGY: The specific name is from Latin *robustus*, “robust,” which refers to the large size of this species among the known species of the genus.

DESCRIPTION

A partial juvenile skull (V17778.1, fig. 6A–C) preserves the premaxilla, the maxilla, the zygomatic process, an incisor, and DP4–M2; it is the basis for the craniomandibular morphology described below.

SKULL: The nasals have been lost in V17778.1. The premaxilla is characterized by a long dorsal process, which extends backward to the middle level of the orbit (fig. 6A). In lateral view the deep premaxilla makes up most of the rostrum anterior to the infraorbital foramen. The suture between the premaxilla and maxilla is simple and straight, and situated anterior to the infraorbital foramen. The premaxilla appears to constitute the anterior half of the rostrum in ventral view, extending from the incisor to P3, and surrounds the anterior portion of the incisive foramen. The interdigitating premaxilla-maxilla suture continues onto the palate and reaches the middle portion of the incisive foramen. The premaxilla and maxilla of *T. robustus* are similar to those of *Hohomys*, but they are higher than in *Cocomys*.

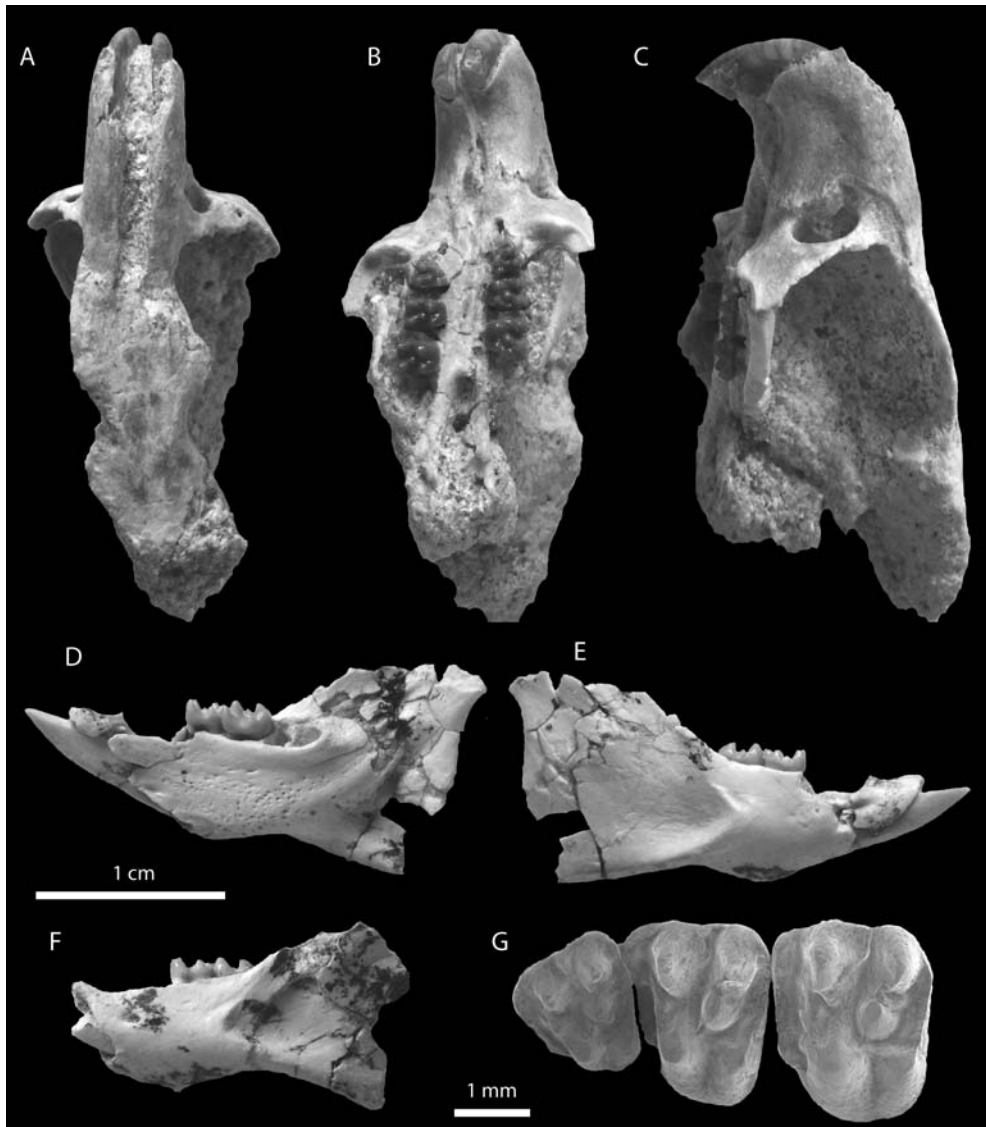


FIG. 6. Partial skull and mandibles of *Tamquammys robustus*. A–C, V17778.1, dorsal, ventral and left lateral views of the skull; D–E, V17772.7, lingual and labial views of the right mandible; F, V17772.2, labial view of the left mandible; G, V17778.1, left DP4–M2 (with the maxillary bone photographically removed). All are to the same scale except G.

The incisive foramen is long and oval and posteriorly positioned (fig. 6B). The length of the foramen is 3 mm, subequal in size to that of *Cocomys* but smaller than that of *Hohomys*. The anterior margin of the foramen is 3 mm posterior to the posterior border of the incisor alveolus, and the posterior margin levels with the anterior part of DP3. The foramen is positioned more posteriorly than those in *Cocomys* and *Hohomys*. The two halves of the incisive foramen are separated by the palatine processes of the premaxillae, which form the entire medial division of the foramina.

The maxilla is a complex bone that contributes to the anterior and ventral edges of the orbit, forms the middle part of the palate and the posterior part of the lateral wall of the nasal cavity, accommodates the infraorbital canal and all the cheek teeth, and bears a strong zygomatic process. In the facial region, the maxilla contacts the premaxilla medially and the frontal and lacrimal posteriorly. The infraorbital foramen is enclosed by the maxilla, and is proportionally larger than those in *Cocomys* and *Hohomys* but significantly smaller than that of *Yuomys* (fig. 6C). The dorsoventral and mediolateral diameters of the infraorbital foramen are 4/1.88 mm, respectively, on the right side of V17778.1, and 3.75/1.57 mm on the left side. In *Exmus* (V7429), the corresponding measurements are 2.5/2.1 mm on the right side and 2.5/2.1 mm on the left side (Wible et al., 2005). In *Hohomys* (V10839), they are 3/2 mm (Hu, 1995). These dimensions are 1.8–2.1 mm dorsoventrally and 1.3–1.7 mm transversely in *Cocomys* (Li et al., 1989). In *Yuomys* the dorsoventral diameter of the infraorbital foramen is 6.4 mm (Li, 1975).

The lachrymal is broken. A distinct nasolachrymal foramen at the anteroventral corner of the lachrymal forms the anterior corner of the orbit above the infraorbital foramen. The diameter of the foramen is 1.25 mm. The anterior surface of the zygomatic root is between DP3 and DP4 and the posterior edge lies at the posterior margin of DP4. A ventral ridge projects from the anterior margin of the zygomatic root, and runs backward along the jugal to mark the attachment area of the anterior portion of the masseter muscle as in *Cocomys*. Such a zygomaseteric structure is similar to the hystricomorph type, but the infraorbital foramen is much smaller than is typical of the hystricomorphous condition. Possibly this form of zygomaseteric structure represents a primitive hystricomorph type.

The frontals are broken and a distinct posterior process is present at a level intermediate between M2 and M3, indicating a large orbit.

The palatal process of the palatine extends anteriorly to a level intermediate between P4 and M1, and posterior to the level of M3. The palatal process bears a posteriorly directed projection (fig. 6B). A pair of posterior palatine foramina is present at the level of the protocone of M1.

MANDIBLE: The ventral edge of the mandible is convex below the cheek teeth, with the ventralmost point situated below m1 (6.5–7 mm) (fig. 6D–F). The diastema is shorter than that of the upper jaw, ranging from 2.4 to 3.2 mm in length. The masseteric fossa is broad and clearly delimited and the dorsal masseteric crest is more distinct than the ventral one. The anterior edge of the fossa is usually at the level of the midpoint of m2 in most specimens (fig. 6E), but occasionally it extends to between m1 and m2 (fig. 6F). On the lateral surface of the jaw are two mental foramina, with the large one anteroventral to p4 and the small one below p4. The angular process lies in the same plane as the cheek teeth and incisor, so that the mandible is typical of sciurognathy.

DENTITION: The cheek teeth increase in size from P4 (p4) to M3 (m3) and are similar to those of *T. wilsoni* in basic morphology, but are significantly larger (fig. 8) and have better-developed cusps and more distinct lophs.

P3 has only one root and its crown is oval in occlusal view (fig. 7I–J). The protocone is distinct and the posterior cingulum is well developed.

DP4 (fig. 7K–L) is molariform, with a distinct paracone and metacone, a well-developed protocone, and a small hypocone. The protoloph extends anterolabially to meet the small paraconule and continues in the same direction toward the anterolingual side of the paracone. The metaconule is distinct, and is connected to the metacone and protocone by a low metaloph. The posterior margin of the tooth is

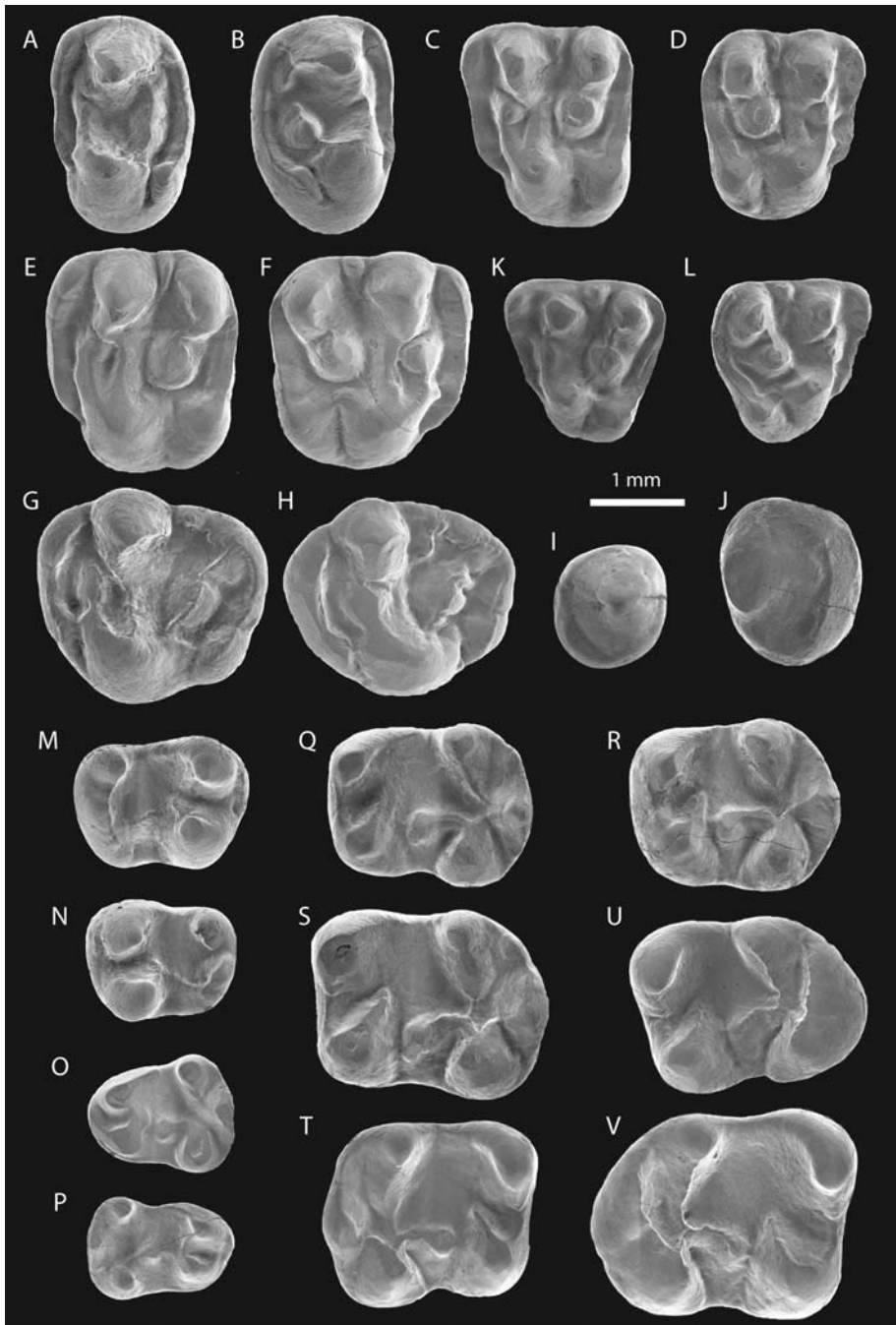


FIG. 7. Cheek teeth of *Tamquammys robustus* in occlusal view. **A**, V17779.127, left P4; **B**, V17779.167, right P4; **C**, V17779.309, left M1; **D**, V17779.353, right M1; **E**, V17779.534, left M2; **F**, V17779.591, right M2; **G–H**, V17779.621, V17779.625, left M3; **I**, V17779.3, left P3; **J**, V17779.30, right P3; **K**, V17779.65, left DP4; **L**, V17779.95, right DP4; **M**, V17780.75, right p4; **N**, V17780.42, left p4; **O**, V17780.2, left dp4; **P**, V17780.28, right dp4; **Q–R**, V17780.108, V17780.125, left m1; **S**, V17780.220, left m2; **T**, V17780.310, right m2; **U**, V17780.360, left m3; **V**, V17780.404, right m3.

formed by a low postcingulum. DP4 differs from the molars in having only one protoloph that connects the protocone to the paraconule, in addition to a well-developed mesostyle.

P4 is double rooted; its crown is compressed anteroposteriorly (wider transversely) to give an oval outline in occlusal view. The tooth is characterized by having two main cusps: the labially situated paracone and the lingually situated protocone (fig. 7A–B). The hypocone is small and not distinct from the postcingulum. The metaconule exceeds the hypocone in size. The precingulum is narrow and long, while the postcingulum is relatively wider.

M1 (figs. 5A, 7C–D) is bunodont and roughly quadrangular in occlusal view. The paracone is subequal to the metacone in size. However, the hypocone is distinctly smaller and lower than the protocone that occupies most of the lingual part of the crown. The metaconule is conical and as large as the metacone. The metaconule forms the main part of the metaloph, which either reaches the protocone or is separated from it by a narrow gap. The protoloph is similar to the equivalent structure in *T. wilsoni*, and has two arms. The precingulum is well developed and joins a distinct parastyle at the anterolabial corner of the tooth. The postcingulum is relatively slender and longer than the precingulum. The small mesostyle is oriented anteroposteriorly. The protocone is connected to the hypocone by a complete entoloph. The sinus is distinct. M1 and M2 are generally similar, but M2 (figs. 5A, 7E–F) differs from M1 in having more distinct cusps and a longer entoloph. In addition, the hypocone of M2 is more labially positioned than that of M1.

The M3 metacone and hypocone are reduced to two swellings on the posterior edge of the tooth. The metaconule is large and conical. The protoloph usually has two lochs (58 of 97) (fig. 7G), but in some teeth it has only a single one that extends to either the paracone or the labial side of the base of the parastyle (39 of 97) (fig. 7H).

The root of the lower incisor extends underneath those of the cheek teeth and ends at a level slightly posterior to m3. The enamel cap of the tooth covers the labial surface and about half of the lingual surface.

The dp4 (figs. 5C, 7O–P) is molariform. The hypoconulid is distinct and contacts the short hypolophid. The mesoconid is distinct and situated on the middle of the low and straight ectolophid.

The p4 (figs. 5B, 7M–N) is nonmolariform, with a trigonid that is higher and wider than those of the molars. The metaconid is the highest cusp. The trigonid basin is open both anteriorly and posteriorly because neither a preprotocristid nor a postprotocristid is present. The talonid of p4 is characterized by a proportionally large entoconid, a weak ectolophid, and absence of a hypolophid and hypoconulid.

The trigonid of m1 is slightly higher, but narrower, than the talonid. The m2 is square in outline. The metaconid is sharp and connected to the blunt protoconid by a low but complete preprotocristid. The postprotocristid is short, so that the trigonid basin is open posteriorly. There are three main cusps on the talonid. The entoconid is highest on lower molars. A distinct hypoconulid is located between the entoconid and hypoconid on m1–2. The ectolophid is distinct and bears a well-developed mesoconid. The hypolophid varies in its shape and direction. In most m1s (13 of 15), the hypolophid extends from the entoconid somewhat posterolabially to the hypoconulid (fig. 7Q–R), but in a few cases (2 of 15) it extends more transversely toward the ectolophid. In contrast, the hypolophid of m2 (21 of 22) usually extends transversely and contacts the ectolophid (fig. 7S–T), but in one tooth it contacts the hypoconulid (1 of 22). We based these counts on teeth that are in situ; we did not include isolated teeth.

The talonid of m3 (fig. 7U–V) is relatively narrower but longer than those of m1 and m2. The hypolophid is transverse and meets the ectolophid.

COMPARISONS

The new specimens from the Eocene beds of the Huheboerhe-Nuhetingboerhe area possess many characters common in early ctenodactyloids, such as a large infraorbital foramen and a sciurognathous mandible. Cheek teeth are brachydont and/or bunodont-lophodont and increase in size distally. P4 and p4 are nonmolariform. Upper molars have a small hypocone that is separated from the protocone by a groove. The trigonid of p4 is higher than the talonid. The hypoconulid is well developed on m1 and m2. On the other hand, the new species has some unique features, such as robust molar cusps and distinct lophs, upper molars with two-armed protolophs, a distinct paraconule present on the anterior protoloph, and the posterior protoloph reaching the base of the paracone. The condition with double protolophs is a characteristic of *Tamquammys*, whereas only a single protoloph is present in other early ctenodactyloids.

Compared to the three previously known species, *Tamquammys robustus* is the largest, with more robust molar cusps and distinct lophs than in other species. The abundant specimens of *T. wilsoni* reported above display a similar tooth morphology as *T. robustus* except for size. Measurements (table 1) of the specimens from AS-1 and AS-2, assigned to the two species, respectively, show that the teeth of *T. robustus* are notably larger than those of *T. wilsoni* (fig. 8). In addition, the p4 talonid of *T. robustus* is wider than that of *T. wilsoni*, and the m1 postprotocristid of *T. robustus* is shorter than that of *T. wilsoni*. The P4 metaconule of *T. tantillus* is isolated and the metaloph is weak, whereas P4 of *T. robustus* has a well-developed metaconule on a distinct metaloph. The hypocone of p4 and the paraconule on the upper molars in *T. dispinorum* are less developed than those in *T. robustus*. The m1 hypolophid of *T. robustus* is oblique and reaches the hypoconulid, whereas those of *T. tantillus* and *T. dispinorum* are more transverse and extend to the ectolophid.

Tamquammys fractus, new species

HOLOTYPE: V17798, a right maxilla with P4–M2, only known specimen (fig. 9).

LOCALITY AND HORIZON: Huheboerhe section, Erlian Basin, Nei Mongol; IM-1, Middle Eocene (fig. 2).

DIAGNOSIS: Larger than *T. tantillus*, *T. wilsoni*, and *T. dispinorum*, but smaller than *T. robustus*. Differs from other known species of *Tamquammys* in having higher cusps, more developed lophs and distinct preparacristae, postparacristae, premetacristae, and postmetacristae on the molars. The M1 and M2 are wide transversely and short anteroposteriorly. The centrocrista is incomplete because the postparacrista is separated from the premetacrista by a notch.

ETYMOLOGY: The specific name is from Latin *fractus*, “broken,” to refer to the incomplete centrocrista.

DESCRIPTION

The protocone and paracone of P4 are distinct and subequal in size. The protocone is connected to the paracone by a complete protoloph. The metaloph extends posterolabially to meet the distinct metaconule and continues in the same direction toward the paracone. A small paraconule is present on the protoloph. The precingulum and postcingulum are low and well developed.

The M1 and M2 are roughly square in occlusal view (fig. 9). They are low crowned and have pronounced cusps and conules and distinct lophs. The protocone, paracone, and metacone are subequal in

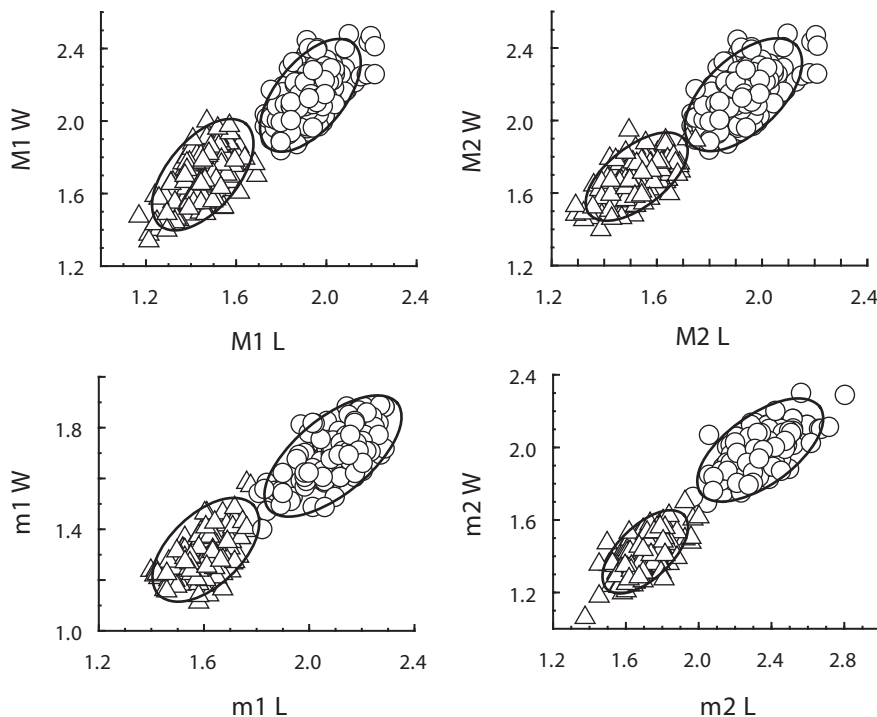


FIG. 8. Comparisons of molar tooth dimensions (in mm) between *T. wilsoni* and *T. robustus* (*T. wilsoni* in triangle and *T. robustus* in circle).

size. A distinct preparacrista and postparacrista form the anterolabial and posterolabial edges of the paracone. The premetacrista and postmetacrista are well developed, but the centrocrista is incomplete because the postparacrista is separated from the premetacrista by a notch. The protoloph also has two arms, an anterior one that ends at a distinct paraconule and a posterior one that is lower and longer than the anterior one. The preparaconule crista is short and extends toward the parastyle. No postparaconule crista is present. The metaconule is larger than the paraconule and is connected to the metacone by an incomplete metaloph. The protocone and metaconule are isolated from each other. The hypocone is low and small, but connected to the protocone by a strong entoloph. The sinus between the protocone and hypocone is distinct. The precingulum is situated anterior to and halfway between the protocone and the paraconule, and extends to the anterolabial corner of the tooth. The postcingulum runs from the hypocone to the posterolabial corner of the tooth.

COMPARISONS

The new specimen from IM-1 possesses characters of *Tamquammys*, including: cheek teeth increase in size distally, P4 is nonmolariform, and there is a distinct but small hypocone on M1–2. There are two protolophs, and connection between the protocone and metaconule is weak on the upper molars.

In *T. fractus* the cusps are higher and the lophs are more developed than in other species of *Tamquammys*. *T. fractus* is larger than *T. tantillus*, *T. wilsoni*, and *T. dispinorum*, but smaller than *T. robustus*. In *T. fractus* the ratio of length to width for both M1 and M2 is smaller than that in *T. wilsoni* and *T. robustus* (L/W of

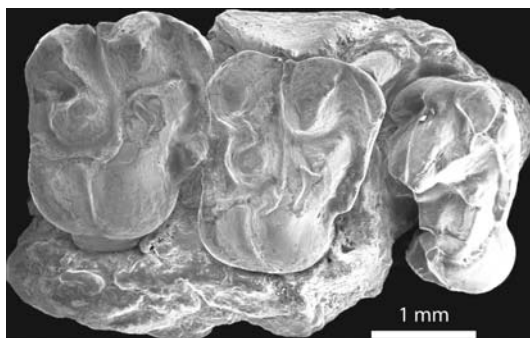


FIG. 9. Occlusal view of a maxillary fragment of *Tamquammys fractus* with P4–M2.

M1: 0.77 in *T. fractus*, 0.85 in *T. wilsoni*, 0.89 in *T. robustus*; L/W of M2: 0.82 in *T. fractus*, 0.9 in *T. wilsoni*, 0.93 in *T. robustus*). There are well-developed postparacristae on the upper molars of some specimens of *T. wilsoni* and *T. robustus*, but the preparacristae, postparacristae, premetacristae, and postmetacristae on M1 and M2 of *T. fractus* are more distinct than in *T. wilsoni* and *T. robustus*. A small, transversely oriented mesostyle is present in the molars of *T. wilsoni* and *T. robustus*, but absent in *T. fractus*.

Tamquammys longus, new species

HOLOTYPE: V16505, an anterior portion of a skull with left DP4, M2–3 and right DP4–M3, only known specimen (fig. 10).

LOCALITY AND HORIZON: Huheboerhe section, Erlian Basin, Nei Mongol; AS-1, Early Eocene (fig. 2).

DIAGNOSIS: Larger than *T. tantillus*, *T. wilsoni*, and *T. dispinorum*. Differs from other Early Eocene ctenodactyloids in having a distinctively long protoloph that extends to the parastyle and the paraconule on M2 and M3 is weak.

ETYMOLOGY: From Latin *longus*, “long,” referring to the long protoloph.

DESCRIPTION

The only known skull of *T. longus* is similar to that of *Tamquammys robustus* (fig. 10A–C). The nasals are broken. The premaxilla has a long dorsal process. The suture between the premaxilla and maxilla is distinctly visible on the right lateral surface of the rostrum anterior to the infraorbital foramen, and continues onto the palate to intersect the incisive foramen about two thirds of the way from the anterior end of this opening. The anterior end of the zygomatic root is at a level between DP3 and DP4, and its posterior surface is level with the posterior margin of DP4. The zygomatic root has a similar extent in *T. robustus*.

The incisive foramen is 3 mm long, similar in size to that of *T. robustus* but smaller than that of *Hohomys*. The anterior edge of the foramen is 3 mm posterior to the posterior border of the incisor alveolus and the posterior border of the foramen is 1.5 mm anterior to the level of the anterior edge of DP3.

The palatal process extends anteriorly to the level of P4 and backward to the front of M3, and is penetrated by two asymmetric pairs of small palatine foramina. The larger anterior palatine foramina lie near the P4/M1 boundary, whereas the smaller posterior ones are medial to M1 and M2. The posterior emargination of the palate is near the level of the anterior part of M3.

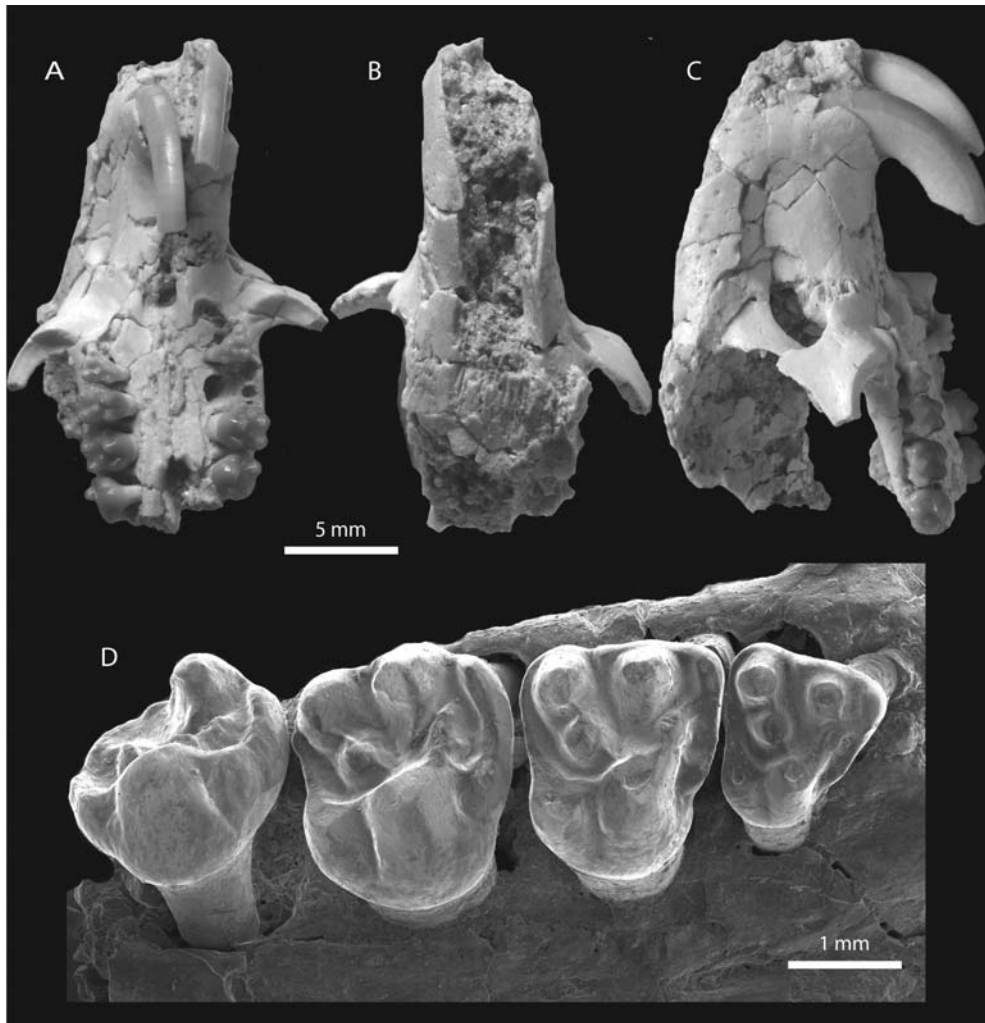


FIG. 10. *Tamquammys longus* (V16505). **A**, ventral view; **B**, dorsal view; **C**, right lateral view; **D**, occlusal view of the right DP4–M3. A–C are to the same scale.

DENTITION: The protocone, paracone, and metacone of DP4 (fig. 10D) are subequal in size, but the hypocone is low and small. There is a small but distinct mesostyle between the paracone and metacone. The protoloph extends toward the parastyle. The metaconule is distinct, and the metacone is connected to the protocone by a low metaloph. The protocone and hypocone are isolated from each other, and the sinus is shallow. A small paraconule is present on the left DP4, but absent on the right.

The upper molars are similar to those of *T. robustus*, except that the protoloph of *T. longus* has only one arm (fig. 10D). The M1 protoloph extends anterolabially to meet a small paraconule and continues toward the parastyle. The paraconule is weakly developed in M2 and M3. The protoloph of M1–2 extends to the anterolingual side of the paracone and the M1–2 sinus is deeper than that of DP4. The entoloph is more distinct in M2 than in M1.

COMPARISONS

Tamquammys longus is based on V16505 from AS-1. Its cranial and dental features show some similarities with known early ctenodactyloids but also have unique features. The skull of *T. longus* resembles that of *T. robustus* in several basic morphological features such as the position, form, and size of the infraorbital foramen, the positions of the anterior and posterior ends of the anterior zygomatic root and the size of the incisive foramen. The relative sizes of the cheek teeth are also similar to those of *T. robustus*. Based on the cranial and dental features the specimen from AS-1 is included in *Tamquammys*. The protoloph typically has two arms in *Tamquammys*, but specimens of *T. wilsoni* reported in this study show that in nearly 8% of specimens the protoloph has one arm. In *T. longus* the protoloph of upper molars that extends toward the parastyle strongly differs from those in other known early ctenodactyloid rodents, including *Cocomys* (Li et al., 1989), *Yuanomys* (Meng and Li, 2010), *Hohomys* (Hu, 1995), *Bandaomys* (Tong and Dawson, 1995), *Viriosomys* (Tong, 1997), *Tsinlingomys* (Li, 1963), *Chuankueimys* (Tong, 1997), *Sharomys*, *Kharomys* (Dashzeveg, 1990a), and *Bumbanomys* (Shevyreva, 1989). The long protoloph is a unique feature that distinguishes *T. longus* from previously known species of *Tamquammys*. The paraconules on M2 and M3 of *T. longus* are weaker than those in *T. tantillus*, *T. wilsoni*, and *T. robustus*. *T. longus* is larger than *T. tantillus*, *T. wilsoni*, and *T. dispinorum*.

Simplicimys, new genus

TYPE SPECIES: *Simplicimys bellus*, sp. nov.

DIAGNOSIS: A small ctenodactyloid. Differs from other Early Eocene ctenodactyloids in having a more distinct connection between the protocone and the metaconule and a U-shaped central basin. Differs from typical *Tamquammys* in having one protoloph. The lower teeth are similar to those of *Tamquammys* (see table 2 for measurements).

ETYMOLOGY: From Latin *simplex* (combining form, *simplici-*), “simple,” referring to the simple structure.

Simplicimys bellus, new species

HOLOTYPE: V16500.1, a left M1 (fig. 11B).

REFERRED SPECIMENS: **AS-5:** V17813.1, left M1; V17813.2–3, left M2; V17813.4–5, right M2; V17813.6–8, left M3. **IM-1:** V16500.2–7, left P4; V16500.8–13, right P4; V16500.14–22, left M1; V16500.23–28, right M1; V16500.29–39, left M2; V16500.40–48, right M2; V16500.49–54, left M3; V16500.55–59, right M3; V16501.1–11, left m1; V16501.12–22, right m1; V16501.23–29, left m2; V16501.30–35, right m2; V16501.36–43, left m3; V16501.44–52, right m3.

LOCALITY AND HORIZONS: Huheboerhe section, Erlian Basin, Nei Mongol; AS-5 and IM-1, Early–Middle Eocene (fig. 2).

DIAGNOSIS: The same as for the genus.

ETYMOLOGY: From Latin *bellus*, “beautiful.”

DESCRIPTION

The occlusal surface of P4 is oval (fig. 11A), being wider than long. P4 is nonmolariform and double rooted. The distinct protocone and paracone are subequal in size. The metacone is usually absent, but

TABLE 2. Measurements of teeth of *Simplicimys bellus* (mm).

	N	Length		Width	
		Min-max	Mean	Min-max	Mean
P4	12	0.9–1.15	1.03	1.4–1.63	1.49
M1	16	1.15–1.45	1.29	1.37–1.54	1.43
M2	20	1.22–1.49	1.33	1.37–1.63	1.49
M3	11	1.22–1.45	1.35	1.24–1.45	1.34
m1	22	1.22–1.53	1.38	1–1.23	1.12
m2	13	1.32–1.55	1.45	1.07–1.31	1.19
m3	17	1.37–1.64	1.51	1.06–1.29	1.17

in rare cases (4 of 12) a small, oval cusp situated posterior to the paracone can be considered an incipient metacone. Posterior to the protocone is a small but distinct hypocone. A small paraconule is present on the protoloph in a few cases (2 of 12), and the metaconule is usually (9 of 12) distinct. The precingulum and postcingulum are well developed, but lower than the protoloph and the short metaloph.

The upper molars are low crowned and triple rooted. M1 is rectangular in occlusal view (fig. 11B), with low crests and four distinct main cusps. The protocone is conical. Although cusps are distinct and crests are generally weak, the protoloph is complete and extends labially to join the paracone. The anterior surface of the loph is steep. A small paraconule, weaker than the metaconule, is present on the protoloph. It has a steep anterior surface but a gently sloped posterior surface. The paracone and metacone are subequal in size. They are lower and more transversely extensive than the protocone. The metacone is connected to the protocone by a low and complete metaloph. The hypocone is more lingually positioned than the protocone, and is connected to the protocone by a low entoloph. The sinus between the protocone and the hypocone is distinct. No mesostyle or mesoloph is present. The protocone, paracone, and metacone, and the crests between these cusps, form a U-shaped central basin. The precingulum is distinct and separated from the protocone and paracone by a shallow groove. The labial end of the precingulum inflates as a small parastyle. The postcingulum is low, and extends labially to the posterior side of the metacone.

M2 is larger than M1, but nearly identical to the latter tooth in morphology. The hypocone of M2 is more labially positioned than that of M1 (fig. 11C).

M3 has a rounded triangular outline in occlusal view, being broader anteriorly than posteriorly (fig. 11D). The protocone is the largest cusp on M3, and the metacone and hypocone are distinctly reduced. The metaloph is shorter than those of M1 and M2, but the entoloph is more distinct.

Each lower molar has two long roots, of which the posterior one is more robust. The trigonid is significantly higher than the talonid. The protoconid and hypoconid are lower than the metaconid and entoconid, respectively.

The m1 is smaller than m2 and tapers anteriorly. The protoconid of m1 is connected to the metaconid by a low preprotocristid and postprotocristid that is complete and connected to the metaconid (fig. 11F) in most teeth (14 of 22), but it is short (fig. 11E) in some teeth (8 of 22). The m1 hypolophid extends from the entoconid to the hypoconulid. The postcingulum is prominent, extending both labially and lingually from the large, cusped hypoconulid. A short and straight ectolophid bears a rounded mesoconid.

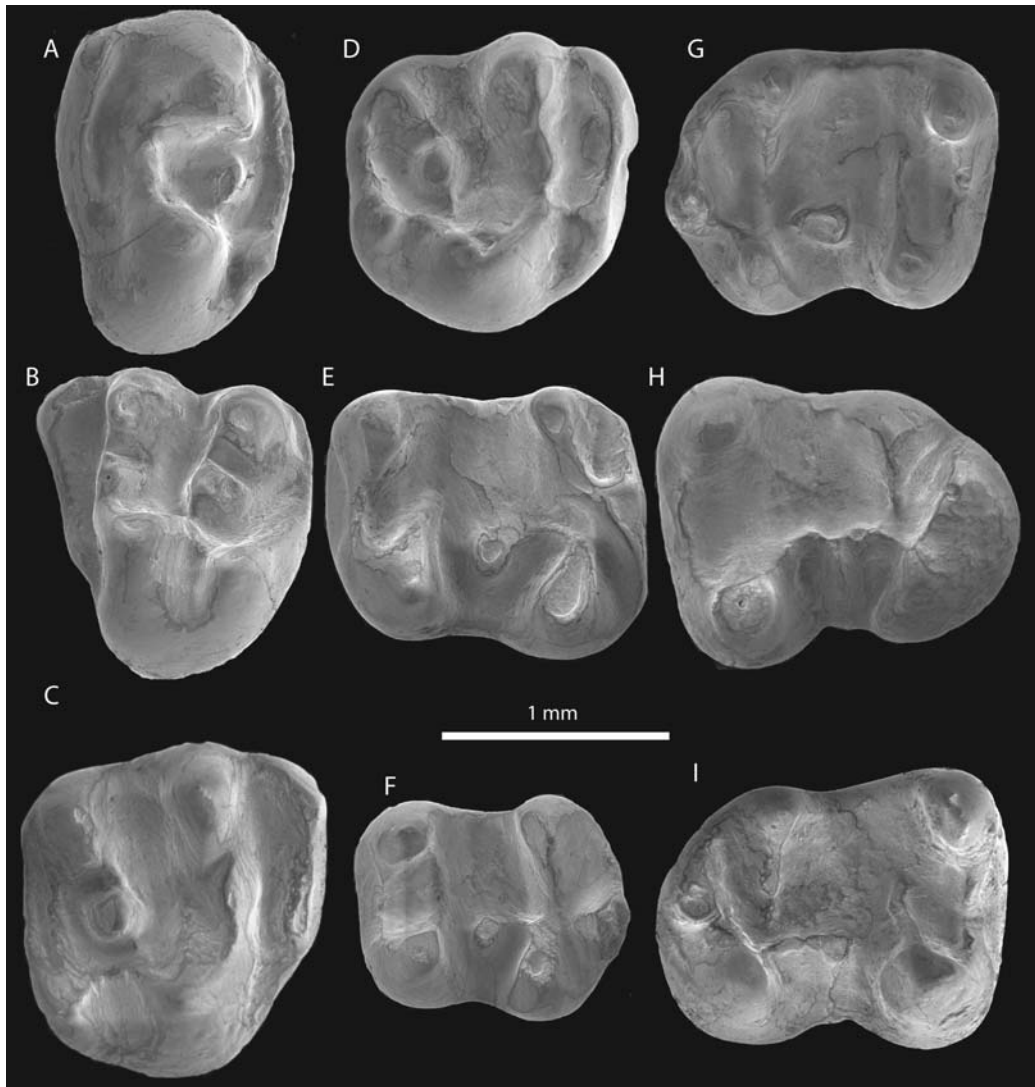


FIG. 11. Cheek teeth of *Simplicimys bellus* in occlusal view. **A**, V16500.5, left P4; **B**, V16500.1, right M1 (holotype); **C**, V16500.45, right M2; **D**, V16500.53, right M3; **E**, V16501.9, left m1; **F**, V16501.4, left m1; **G**, V16501.31, right m2; **H**, V16501.39, left m3; **I**, V16501.44, right m3.

The postprotocristid of m2 is short in some teeth (5 of 13), leaving the trigonid basin open. The hypolophid of m2 extends transversely to the hypoconid (fig. 11G), but that of m3 is concave anteriorly and in contact with the ectolophid in front of the hypoconid. The hypoconulid of m3 is weaker than those of m1 and m2, and is incorporated into a postcingulum. The m3 ectolophid is longer than those of m1 and m2. An ectomesolophid is present in a few specimens (7 of 17) (fig. 11H).

COMPARISONS

The distinction between a molariform and nonmolariform P4 is a taxonomically important character among ctenodactyloids. Because the new species has a nonmolariform P4, we compare it only with

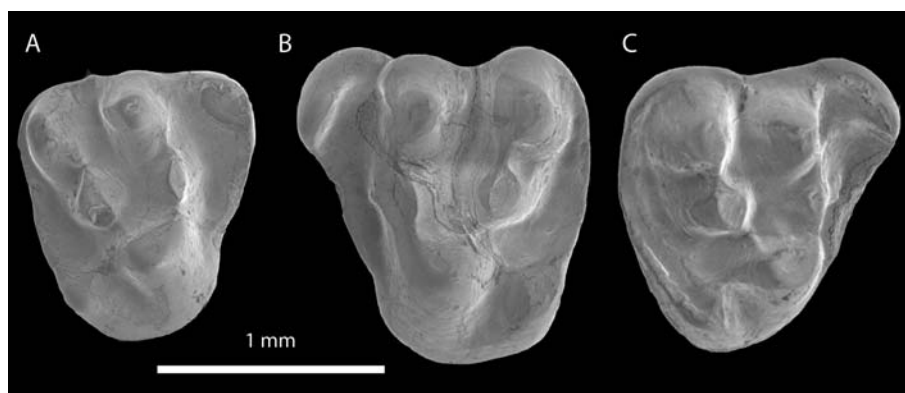


FIG. 12. Cheek teeth of *Yongshengomys extensus* in occlusal view. A, V16504.4, right DP4; B, V16504.1, left M1 (or M2; holotype); C, V16504.25, right M1 (or M2).

early ctenodactyloid rodents known from Asia that share this characteristic. Those having a molariform P4, such as yuomyids, chapattimyids and *Advenimus*, are not considered here. *Simplicimys* is from the AS-5 and IM-1, and later than the age of *Cocomys*, *Yuanomys*, *Bandomys*, and *Exmus*.

Based on cranial and dental features, *Cocomys lingchaensis* (Li et al., 1989) has been considered representative of the most primitive rodents and has often been placed at the base of the clade Rodentia in phylogenetic analyses (Meng et al., 2003; Asher et al., 2005). *Cocomys* differs from *Simplicimys* in having more conical cusps on upper molars, a larger mesostyle, a short postprotocristid, and no hypoconid on m1-2. In contrast, *Simplicimys* has a distinct metaconule and a small hypocone on P4. The molars of *Simplicimys* have better-developed crests, the paraconule on M1 is small but distinct, and the postprotocristid of m1 and the hypolophids of the lower molars are also distinctly developed.

Yuanomys zhoui was reported from the Bumbanian *Gomphos* bed (NM-3) in the Erlian Basin, Nei Mongol, China (Meng and Li, 2010). *Yuanomys* has slim and isolated cusps and conules on the cheek teeth, and a transversely expanded paracone and metacone with steep surfaces that face a broad trigon basin. *Simplicimys* differs from *Yuanomys* in having more distinct crests, particularly the distinct proto-loph, conical cusps, and a weaker paraconule.

The protoloph of each upper molar of *Tamquammys* has two arms, and in most specimens of *Tamquammys* the paraconule, metaconule, and mesostyle of each upper molar are distinct. In *Simplicimys* only a single protoloph is present, the mesostyle is absent, and the metaloph is more complete than in *Tamquammys*.

Viriosomys jingweni (Tong, 1997) differs from *Simplicimys* in having a weak paraconule, a reduced metaconule, a short entoloph, and a narrow and shallow sinus of M1-2.

Tsinlingomyinae was established by Tong (1997) and includes two species: *Tsinlingomys youngi* (Li, 1963) and *Chuankueimys xichuanensis* (Tong, 1997). *Simplicimys* is smaller than *Tsinlingomys* and *Chuankueimys*. The differences between them are as follows: precingulum shelf on P4 of *Tsinlingomys* and *Chuankueimys* wide and extended labially; each upper molar of *Tsinlingomys* and *Chuankueimys* with poorly developed entoloph and hypocone small and situated near protocone; hypolophid on m1-2 of *Tsinlingomys* curved posteriorly and contacting hypoconulid; and hypolophid on m1-2 of *Chuankueimys* extending transversely, but end of hypolophid bends posteriorly and contacts hypoconulid. In *Sim-*

plicimys the mesoconid is prominent and the ectomesolophid on m3 is sometimes distinct, but both features are absent in *Tsinlingomys* and *Chuankueimys*.

Hohomys lii was named by Hu (1995) for a specimen comprising the anterior part of a skull and associated lower jaws with complete upper and lower dentitions, from the Yuhuangding Formation near Wangjiazhai Village, Xijiadian Town, Hubei. *Simplicimys* is smaller than *Hohomys*. The connection between the protocone and metaconule of M1–2 is better developed in *Simplicimys* than in *Hohomys*. In *Hohomys*, the hypolophid of m1–2 is a short crest extending towards (but not reaching) the hypoconulid, and no hypolophid is present on m3; *Simplicimys*, in contrast, has a distinct and transverse hypolophid on m2–3.

Two skulls and associated mandibles from the Yuhuangding Formation of Hubei Province were described as *Exmus mini* (Wible et al., 2005). *Exmus* is larger than *Simplicimys*. *Exmus* also differs from *Simplicimys* in several features of the cheek teeth, including the absence of a paracone, the lack of a connection between the protocone and the metaconule on M1–2, and the absence of a postprotocristid or hypolophid of each lower molar.

Hannanomys was established by Guo et al. (2000) based on an incomplete right mandible from Jun County in Hubei Province. *Simplicimys* can be clearly distinguished from *Hannanomys* by the following characters: on m2, longer postprotocristid and more transverse hypolophid that contacts the ectolophid; longer ectolophid that extends to the protoconid on m1–3; and smaller size.

The type series of *Bandaomys zhonghuaensis* preserves P4–M2, p4–m1 and a few isolated cheek teeth (Tong and Dawson, 1995). M1 has a more robust paraconule and a weaker parastyle in this specimen than in *Simplicimys*. The lower cheek teeth of *Bandaomys* have weakly developed hypoconulids and hypolophids. The entoloph and sinus of each upper molar are weaker in *Bandaomys* than in *Simplicimys*.

Two ctenodactyloid rodents, *Mergenomys orientalis* and *Butomys prima*, have been described from middle Eocene localities of the eastern Gobi Desert of Mongolia (Dashzeveg and Meng, 1998). *Mergenomys* differs from *Simplicimys* in several features of the cheek teeth, including absence of entoloph between protocone and hypocone, absence of paraconule, large metaconule isolated from protocone and large hypocone, more lingually positioned ectolophid, absence of mesoconid, and weak hypolophid. Only lower teeth are known for *Butomys*. The ectolophid on m1–2 of *Butomys* is very weak, extending along the midline of the tooth, and the hypoconulid is isolated from both the hypoconid and the entoconid.

Adolomys ameristus, *Tsagankhushumys onos*, *T. deriphatus*, *Bumbanomys edestus*, and *Esesempomys centralasiae* were all described by Shevyreva (1989) from strata of the Bumban Member of the Naran-Bulak Formation exposed at the Tsagan Khushu locality, Mongolia. More complete and diverse ctenodactyloid material from the same locality was described by Dashzeveg (1990a), who established *Sharomys singularis*, *S. parvus*, *Kharomys mirandus*, *Kh. gracilis*, *Tsagamys subitus*, *Ulanomys mirificus*, and *Boromys grandis*. Averianov (1996) suggested that some of the species described from the Bumban Member were synonymous, but considered *Tsagankhushumys deriphatus* (= *T. onos* = *Bumbanomys edestus* = *Sharomys singularis* = *S. parvus* = *Kharomys mirandus* = *Ulanomys mirificus*) to be a valid taxon from the Tsagan Khushu locality. M. Dawson also considered (personal commun.) some species from the Bumban Member to be nomina nuda or junior synonyms of other taxa. Revising the taxonomy of the rodents from the Bumban Member of Tsagan Khushu is well beyond the scope of the present study, and we do not anticipate that any other substantial revision of these rodents will be carried out in the near

future, as pointed out by Meng and Li (2010). In this study we make a general comparison with the teeth of rodents from the Bumban Member, rather than comparing *Simplicimys* with each of the named Bumban species, which is beyond our ability. Our comparisons show that all upper molars known from the Bumban Member have more expanded cusps and conules than are present in *Simplicimys*, and less-developed crests between the cusps and conules. The lower teeth have a short hypolophid or none at all. All of them are generally larger than the corresponding teeth of *Simplicimys*.

Alaymys ctenodactylus was described from the Early Eocene locality Andarak 2 in Kyrgyzstan (Averianov, 1996). The genus differs from *Simplicimys* in having a transversely elongate and short crown, a less developed parastyle of M1–2, a longer postprotocristid, and a closed trigonid basin on lower molars.

Juniperimus flerovi from the Chakpaktas Formation of the Zaisan Depression (eastern Kazakhstan) was described by Shevyreva (1996). The metaloph of M2 of *Juniperimus* is almost parallel to the protoloph and completely separated from the protocone. The hypoconulid of m2 is connected to the hypocone, but not to the entolophid. The ectolophid is almost central on m1, and curves lingually on m2. *Simplicimys* is smaller than *Juniperimus*. The metaloph of M1–2 of *Simplicimys* contacts the protocone, and the hypolophid and ectolophid of each lower molar are more distinct than in *Juniperimus*.

Yongshengomys, new genus

TYPE SPECIES: *Yongshengomys extensus*, sp. nov.

DIAGNOSIS: A small ctenodactylid. Differs from most ctenodactylids in having a hypertrophic parastyle, a labially extended precingulum shelf and a hypocone that is more lingually positioned than the protocone (fig. 12; see table 3 for measurements).

ETYMOLOGY: In honor of Yongsheng Tong, who has made a great contribution to the study of Paleogene mammals of China, including rodents.

Yongshengomys extensus, new species

HOLOTYPE: A left M1 (or M2) (V16504.1) (fig. 12B).

REFERRED SPECIMENS: V16504.2–9, left DP4; V16504.10–16, right DP4; V16504.17–22, left M1 (or M2); V16504.23–25, right M1 (or M2).

LOCALITY AND HORIZON: Huheboerhe section, Erlian Basin, Nei Mongol; IM-1, Middle Eocene (fig. 2).

DIAGNOSIS: The same as for the genus.

ETYMOLOGY: From Latin *extensus*, “extended,” to refer to the labially extended precingulum.

DESCRIPTION

The teeth are somewhat cuneiform in occlusal view and have distinct cusps but weak crests (fig. 12). The protocone is comma shaped, and the paracone and metacone are conical and subequal in size. The hypocone is smaller than the other three main cusps and situated more lingually than the protocone. The protoloph and metaloph are usually distinct and contact the protocone, but the metaloph is not connected to the protocone in some teeth (5 of 25). The metaconule is slightly smaller than the metacone, and distinctly larger than the paraconule that is present on the protoloph. The entoloph is weak and the sinus is

TABLE 3. Measurements of teeth of *Yongshengomys extensus* (mm).

Tooth	N	Length		Width	
		Min-max	Mean	Min-max	Mean
DP4	15	1-1.15	1.07	1.03-1.25	1.16
M1 (or M2)	10	1.09-1.28	1.19	1.16-1.4	1.27

distinct and deep. The precingulum is wide, and rises to form a distinct parastyle at the labial extended precingulum shelf. The precingulum is separated from the protocone by a shallow groove. The postcingulum is low and extends labially to the posterior side of the metacone. No mesostyle is present.

DP4 and M1 (or M2) can be differentiated by the presence of a contact facet on the anterior surface. A small and weak surface on DP4 suggests the presence of a DP3 that is usually small and has a simple structure in primitive ctenodactyloid. The surface is larger and more distinct on M1 (or M2). Teeth identified as examples of DP4 are smaller than those identified as examples of M1 (or M2), and the hypocone of DP4 is more lingually placed than that of M1 (or M2).

COMPARISONS

In our collection, specimens of *Yongshengomys extensus* are relatively few, but they display distinctive dental morphologies. They differ from most ctenodactyloids mainly in an inflated parastyle that projects anteriorly at the anterolabial corner of the molar. The precingulum is weak anterior to the protocone, but expands labially to form a shelf that is confluent with the large parastyle. In addition, the hypocone, although smaller than the protocone, is more lingually positioned than the protocone.

Tsinlingomys youngi, *Chuankueimys xichuanensis*, and *Zoyphiomys sinensis* were described from the Hetaoyuan Formation of Xichuan County of Henan Province (Tong, 1997). Although *Yongshengomys* is similar to these taxa in having a distinct precingulum shelf, it also clearly differs from them. *Yongshengomys* is smaller than *Tsinlingomys* and *Chuankueimys*. In *Tsinlingomys* and *Chuankueimys*, the protoloph and metaloph of M1-2 are better developed than in *Yongshengomys* and the hypocone of each upper molar is positioned more labially. *Yongshengomys* differs from *Z. sinensis* in having a longer protoloph, a more distinct paraconule, a smaller and lower hypocone, and a more extended precingulum shelf of P4-M2.

Ekatherinomys mamma was named and described by Shevyreva (1996) on the basis of a single tooth (P4) from the Zaisan Depression of eastern Kazakhstan. *Ekatherinomys* has a lingual hypocone, and a massive and distinct precingulum shelf. *Ekatherinomys* differs from *Yongshengomys* in the following features: a transversely elongated metacone, and a metaconule connected to the mesostyle, which in turn joins the labial side of the base of the metacone.

The hypocone of *Chapattimys* (Hussain et al., 1978; Hartenberger, 1982) from Pakistan is more lingually placed and similar in position to that of *Yongshengomys*. *Chapattimys* differs from *Yongshengomys* in having a better-developed hypocone on M1 and M2, a more distinct mesostyle, and a precingulum shelf that does not expand labially or form a parastyle.

Orogomys obscurus was described from the Bumban Member of the Naran-Bulak Formation in the Nemeget Basin of Mongolia by Dashzeveg (1990b). *Orogomys* is similar to *Yongshengomys* in that M1-2 each has an approximately triangular outline, and in that the parastyle is massive and distinct. However,

there are also important differences between the two taxa. In *Yongshengomys*, the paraconule is weak, no mesostyle is present, and the hypocone is more lingual in position. In *Orogomys*, the protoloph and metaloph of M1–2 are less well developed and the paracone is isolated from the paraconule.

Yuomys Li, 1975

Yuomys huheboerhensis, new species

HOLOTYPE: A left M1 (V17803.1) (fig. 13B).

REFERRED SPECIMENS: V17803.2, left P4; V17803.3–4, left M1; V17803.5–6, right M1; V17803.7–8, right M2; V17803.9, left M3; V17804.1–2, right m1; V17804.3, left m2; V17804.4–5, right m2; V17804.6–7, left m3; V17804.8, right m3.

LOCALITY AND HORIZON: Huheboerhe section, Erlian Basin, Nei Mongol; IM-1, Middle Eocene (fig. 2).

DIAGNOSIS: Differs from other known species of *Yuomys* in being smaller and having molars that are approximately as long as they are wide (see table 4 for measurements). Differs from *Y. cavioides* and *Y. weijingensis* in lacking a mesostylid and a conule on the hypolophid. Differs from *Y. elegans* in having a short precingulum, and a better-developed preprotocristid and hypoconulid. Differs from *Y. minggangensis* and *Y. yunnanensis* in having a more transverse hypolophid that meets the ectolophid at a point anterior to the hypoconid on m1 and m3, but at the hypoconid on m2.

ETYMOLOGY: The specific name is derived from Huheboerhe, the type locality for the species.

DESCRIPTION

The upper cheek teeth are bunodont, but approach a four-crested pattern. P4 is larger than M1. P4 lacks a hypocone, but has a prominent protocone (fig. 13A). The paracone is isolated from, and slightly higher than, the metacone. The protoloph is complete and transverse, with no indication of a paraconule. The incomplete metaloph, ending near the large metaconule runs parallel to the protoloph. The precingulum is shorter than the postcingulum.

M1 and M2 are quadrangular. On these teeth the four main cusps are prominent, the crests are low, and the paracone and metacone are subequal in size and widely separated from one another (fig. 13B–C). The hypocone is well developed, being only slightly smaller than the protocone and separated from it by a distinct sinus extending from the occlusal surface halfway toward the base of the crown. The protoloph is complete, extending from the protocone to the paracone. No paraconule is present, but the metaconule is large, being subequal to the metacone in size. The metacone is connected to the metaconule by a short metaloph that converges toward, but fails to contact the protocone. The precingulum begins anterolabial to the protocone and extends to the anterolabial corner of the tooth, where a distinct parastyle is present in some cases (1 of 3). The postcingulum is narrow and runs from the hypocone to the posterolabial side of the metacone. The mesostyle is weak or absent.

M2 is similar to, but larger than, M1. On M3 the metacone is reduced, and the hypocone is labially positioned and smaller than those of M1 or M2. A distinct mesostyle is present on M3 (fig. 13E), and the metaloph of this tooth is complete and extends to the protocone.

The m1 is smaller than m2 and tapers slightly anteriorly. The trigonid of m1 is higher than the talonid (fig. 13F–G). The protoconid is larger than the metaconid, and the protoconid is higher than the

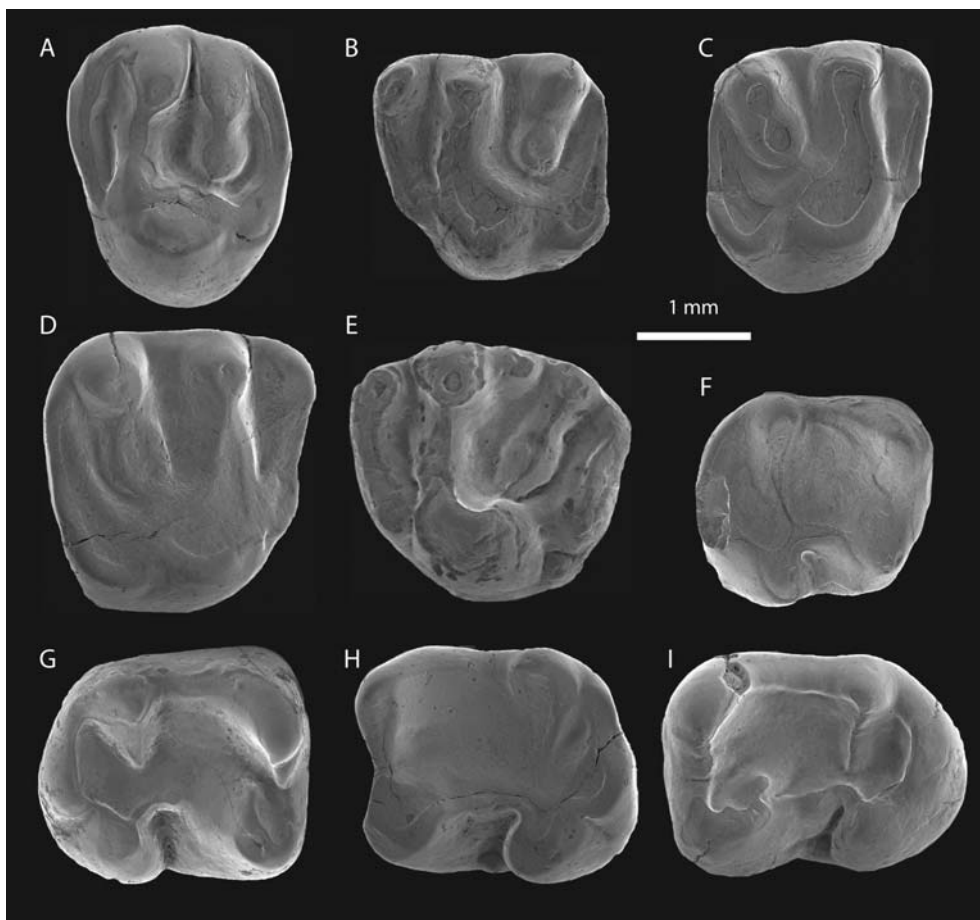


FIG. 13. Cheek teeth of *Yuomys huheboerhensis* in occlusal view. **A**, V17803.2, left P4; **B**, V17803.1, left M1; **C**, V17803.6, right M1; **D**, V17803.8, right M2; **E**, V17803.9, left M3; **F**, V17804.2, right m1; **G**, V17804.1, right m1; **H**, V17804.3, left m2; **I**, V17804.7, left m3.

latter on the worn m1. The preprotocristid is low, but connects the protoconid to the metaconid. The postprotocristid is short, so that the trigonid basin is not fully enclosed. A complete, transversely aligned hypolophid is present on the talonid basin, and contacts the ectolophid at a point anterior to the hypoconid. There is a distinct hypoconulid on the postcingulum. The hypoconid is connected to the protoconid by a complete ectolophid. No mesostylid or mesoconid is present.

The m2 is similar to m1 (fig. 13H). The postprotocristid is weakly developed in one tooth (1 of 3). The hypolophid contacts the hypoconid and is positioned generally farther posteriorly than the hypolophid of m1.

The m3 has a weak hypoconulid, a distinct mesoconid (fig. 13I), and an ectomesolophid (1 of 3) in some cases.

COMPARISONS

The specimens of *Yuomys huheboerhensis* from IM-1 in the Huheboerhe section differ from ctenodactyloids such as *Tamquammys wilsoni*, *T. fractus*, *Simplicimys bellus*, and *Yongshengomys extensus* in the same

TABLE 4. Measurements of teeth of *Yuomys huheboerhensis* (mm).

	N	Length		Width	
		Min-max	Mean	Min-max	Mean
P4	1	2	2	2.5	2.5
M1	5	1.75-2.1	1.91	1.7-2.25	1.95
M2	2	2.4	2.4	2.5-2.6	2.55
M3	1	2.5	2.5	2.3	2.3
m1	2	2.4-2.1	2.25	1.9-2.1	2
m2	3	2.5-2.6	2.53	2-2.2	2.1
m3	3	2.7-3	2.83	2-2.2	2.1

beds. *Y. huheboerhensis* is larger than *Tamquammys wilsoni*, *Simplicimys bellus*, and *Yongshengomys extensus*. It also differs from the three taxa in having a distinct metacone on P4, a well-developed hypocone on M1 and M2, and metaloph directed toward but never in contact with protocone on M1-2. The m1 hypolophid of *Tamquammys wilsoni* and *Simplicimys bellus* is oblique and reaches the hypoconulid, whereas that of *Y. huheboerhensis* is more transverse and extends to the ectolophid. In *Yongshengomys*, the precingulum expands labially to form a shelf and is better developed than in *Y. huheboerhensis*.

Yuomys includes five previously described species: *Y. cavioides*, *Y. eleganes*, *Y. minggangensis*, *Y. weijingensis*, and *Y. yunnanensis*.

Y. cavioides was named and described by Li (1975) based on specimens from Mianchi and Jiyuan counties in Henan Province and Ula Usu in Nei Mongol. *Y. huheboerhensis* is smaller than *Y. cavioides*; its M1 and M2 are both approximately as long as wide in occlusal view. The sinus of each upper molar is deeper in *Y. cavioides* than in *Y. huheboerhensis*. *Y. cavioides* possesses a small conule on the hypolophid, increasing in size from m1 to m3, and a distinct mesostylid. In *Y. huheboerhensis* the mesostylid and the conule on the hypolophid of m1-3 are absent, but the distinct mesoconid and incipient ectomesolophid both are present only on m3.

Y. eleganes from the Litugou Formation of the Upper Eocene of Tongbai County, Henan Province, was described by Wang (1978). *Y. eleganes* differs from *Y. huheboerhensis* in several aspects of the cheek teeth, including larger size, longer precingulum of each upper molar, metaconid anterior to protoconid on m2 and m3, protoconid isolated from metaconid, and weak hypoconulid of m1-3.

Y. weijingensis was established by Ye (1983) based on an incomplete left maxilla with M1-2 and an isolated m2 from the Upper Eocene of the Ulan Shiren area, Nei Mongol. In M1-2 of *Y. weijingensis* the parastyle is distinct and the metaloph extends to the base of the protocone. In upper molars of *Y. huheboerhensis*, by contrast, the parastyle is weak or absent and the metaloph never contacts the protocone. In addition, the lower teeth of *Y. huheboerhensis* differ from the m2 of *Y. weijingensis* in a more transverse hypolophid, and lack of mesostylid and conule on the hypolophid.

Y. yunnanensis was from the Upper Eocene of the Chake area, Jianshui County, Yunnan Province (Huang and Zhang, 1990). *Y. minggangensis* was named based on a fragmentary lower jaw with p4-m1 from the Pingchangguan Basin of Henan Province (Wang and Zhou, 1982). *Y. yunnanensis* and *Y. minggangensis* differ from *Y. huheboerhensis* in their larger size and in that m1 has a straight hypolophid that extends to the hypoconid. The postprotocristid on m1-2 of *Y. yunnanensis* is long and contacts the base of the metaconid.

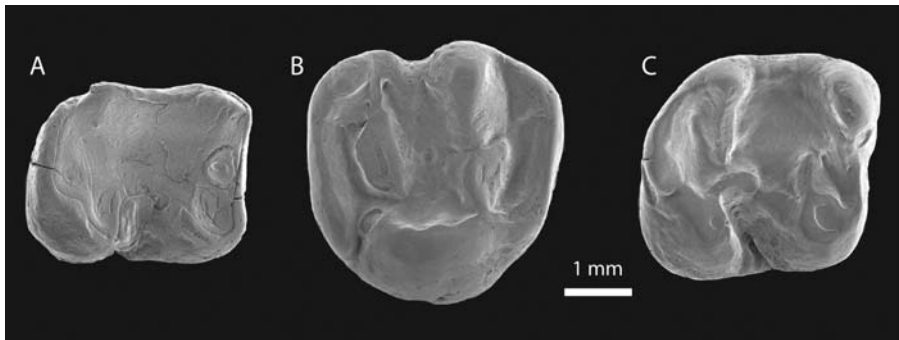


FIG. 14. **A**, right m1 or m2 of *Yuomys* sp. A (V17805); **B**, right M3 of *Yuomys* sp. B (V17806); **C**, right m3 of *Yuomys* sp. C (V17807).

In general, *Y. huheboerhensis* is smaller than other known species of *Yuomys* (table 5), and has morphologically simpler teeth that lack a mesoconid on m1–2, a mesostylid and a conule on the hypolophid.

Yuomys sp. A

SPECIMEN: A right m1 (or m2) (V17805) (fig. 14A).

LOCALITY AND HORIZON: Huheboerhe section, Erlian Basin, Nei Mongol; IM-1, Middle Eocene (fig. 2).

DESCRIPTION AND COMPARISONS

The tooth measurement (length/width in mm) is 3/2.4. This tooth can be identified as m1 or m2 by the presence of contact facets on the anterior and posterior surfaces. The preprotocristid and postprotocristid extend from the protoconid to the anterior and posterior sides of the metaconid. A small trigonid basin is present between the two ridges. The hypolophid contacts the ectolophid at a point anterior to the hypoconid. The hypoconulid is weak. There is no mesoconid or mesostylid. The specimen resembles *Yuomys* in having a complete ectolophid and transverse hypolophid, but differs from known species of the genus in having a better-developed postprotocristid and a closed trigonid basin. Here this tooth is tentatively referred to *Yuomys*, but considered presently indeterminate at the specific level.

Yuomys sp. B

SPECIMEN: A right M3 (V17806) (fig. 14B).

LOCALITY AND HORIZON: Huheboerhe section, Erlian Basin, Nei Mongol; IM-1, Middle Eocene (fig. 2).

DESCRIPTION AND COMPARISONS

This tooth measurement (length/width in mm) is 3.4/3.5. On this tooth the protocone is the largest cusp. The hypocone is reduced, and more labially positioned than the protocone. The paracone is higher than the metacone. A distinct paraconule is present on the complete protoloph. A large metaconule is connected to the metacone by a short metaloph, but is isolated from the protocone. The precingulum with a small parastyle and the postcingulum are distinct. No mesostyle is present.

TABLE 5. Measurements of cheek teeth of various species of *Yuomys* (mm).

	<i>Y. huheboerhensis</i> , sp. nov.	<i>Y. cavioides</i>	<i>Y. elegans</i>	<i>Y. minggangensis</i>	<i>Y. weijingensis</i>	<i>Y. yunnanensis</i>
P4(L)	2	3.8–4.2	—	—	—	—
P4(W)	2.5	3.75–4.2	—	—	—	—
M1(L)	1.75–2.1	3.2–4.15	—	—	3.5	—
M1(W)	1.7–2.25	3.75–4.2	—	—	3.6	—
M2(L)	2.4	3.45–4.1	3.3	—	3.37	—
M2(W)	2.5–2.6	3.85–4.4	3.9	—	4.17	—
M3(L)	2.5	4.35	—	—	—	—
M3(W)	2.3	4.25	—	—	—	—
p4(L)	—	3.9–4.55	4	—	—	—
p4(W)	—	3.8–3.95	3.5	—	—	—
m1(L)	2.1–2.4	3.55–3.85	3.3–3.5	4.1	—	3.25
m1(W)	1.9–2.1	3.15–3.45	3.2	4	—	3.15
m2(L)	2.5–2.6	3.55–4.2	3.5	—	3.83	3.65
m2(W)	2–2.2	3.4–3.7	3.2–3.6	—	3.7	3.6
m3(L)	2.7–3	4.45–5	4.8	—	—	—
m3(W)	2–2.2	3.6–4.35	4.8	—	—	—

Y. huheboerhensis and *Y. cavioides* are known species of *Yuomys* that preserve M3. This new specimen from IM-1 differs from *Y. huheboerhensis* in being larger and in having a more distinct paraconule and a reduced hypocone on M3. The specimen differs from *Y. cavioides* in having a less well-developed precingulum and a more reduced hypocone. As a single isolated tooth, the new specimen can only be tentatively attributed to *Yuomys*, and remains indeterminate at the specific level.

Yuomys sp. C

SPECIMEN: A right m3 (V17807) (fig. 14C).

LOCALITY AND HORIZON: Huheboerhe section, Erlian Basin, Nei Mongol; IM-1, Middle Eocene (fig. 2).

DESCRIPTION AND COMPARISONS

This tooth measures (length/width in mm) 3.2/3. On it the preprotocristid is low, but pronounced. The postprotocristid is short, and the trigonid basin is open posteriorly. The transverse hypolophid extends to the complete ectolophid. A distinct hypoconulid is present on the postcingulum. A small mesostylid is present between the metaconid and the entoconid. Compared to *Y. cavioides*, this new specimen from IM-1 is smaller, has a weaker postprotocristid, and lacks a conule on the hypolophid. Differences from *Y. huheboerhensis* include larger size, a more distinct hypoconulid and mesostylid, and the lack of a mesoconid or ectomesolophid. The new specimen differs from *Y. elegans* in being smaller, with the metaconid located no farther anteriorly than the protoconid, and in the short postprotocristid with more distinct mesostylid.

Advenimus Dawson, 1964*Advenimus ulungurensis* Meng et al., 2001

HOLOTYPE: IVPP V12674, partial right and left lower jaw with broken incisors, lateral half of the right p4, complete right m2–3, left m1, left P4, and left M2 from a single individual organism (Meng et al., 2001).

REFERRED SPECIMENS: Two left mandibles with p4–m3 (V16499, V16506) (fig. 15; table 6).

LOCALITY AND HORIZONS: The holotype is from the late Early Eocene Ulunguhe Formation of Sa-er-duo-yi-la, Xinjiang. The referred specimens are from the AS-5 in the Huheboerhe section of the Huheboerhe-Nuhetingboerhe area, Erlian Basin, Nei Mongol, which is considered late Early Eocene (fig. 2).

EMENDED DIAGNOSIS: A medium-sized ctenodactyloid; cheek teeth low crowned; lower cheek teeth increasing in size posteriorly; P4/p4 submolariform; P4 precingulum distinct; P4 metacone and paracone well developed but closely placed to each other, both cusps connected to the protocone with complete protoloph and metaloph; M2 precingulum distinct; masseteric fossa broad and extending anteriorly to level of trigonid of m2; p4 talonid wider than trigonid; p4 protoconid and metaconid isolated from each other; p4 hypoconulid distinct; molar preprotocristid complete and a weak hypolophid leading to the anterior base of the hypoconulid; ectolophid low but complete; and mesoconid weak, but mesoconid and ectomesolophid occasionally present on m3.

DESCRIPTION

Two left incomplete mandibles with p4–m3 are preserved. The masseteric fossa of V16499 (fig. 15C) is broad and its anterior edge is at the level of the trigonid of m2. The lower incisor, as shown by a cross section revealed by breakage in V16499, is transversely narrow. The last lower premolar of V16506 has undergone considerable postmortem damage, obliterating the protoconid and metaconid (fig. 15B). The p4 of V16499 are significantly narrower anteriorly than posteriorly (fig. 15A–B). A distinct hypoconulid is present on the talonid, and no hypolophid is present. The morphology of V16506 suggests that the premolar is probably dp4.

The protoconid and metaconid of p4 are conical and separated from each other by a longitudinal groove (fig. 15A). The metaconid is located farther anteriorly than the protoconid. The talonid is shorter than the trigonid and bears three cusps. The hypoconulid is distinct and compressed anteroposteriorly to form a transverse ridge. The ectolophid is low but complete. Neither a hypolophid nor a mesoconid is present.

The metaconid is the highest cusp on m1, and lies slightly anterior to the protoconid. The anteroposteriorly orientated trigonid basin is narrow and closed anteriorly by a low preprotocristid. The hypoconid is larger than the entoconid. The hypoconulid is the same shape as that on p4. The short hypolophid extends to the anterior side of the base of the hypoconulid. A small mesoconid is present on the low ectolophid. The m2 is significantly larger than m1, and has more robust cusps. The hypolophid of m2 is shorter than that of m1.

The m3 is the largest cheek tooth (fig. 15A–B). Its metaconid extends farther anteriorly than those of the other cheek teeth. The postprotocristid of m3 of V16499 is longer than those of m1 and m2. No

TABLE 6. Measurements of lower teeth of *Advenimus* (mm).

		<i>A. burkei</i> (Dawson, 1964)	<i>A. hupeiensis</i> (Dawson et al., 1984)	<i>A. ulungurensis</i> (Meng et al., 2001)	<i>A. ulungurensis</i> (V16499)	<i>A. ulungurensis</i> (V16506)
p4	L	2	2.15	2.4	2.25	2.5
	W	1.4	1.9	1.88	1.88	1.9
m1	L	2.1–2.3	2.1–2.45	2.31–2.42	2.41	2.5
	W	1.8	1.8–2	1.84–2	2.03	2.1
m2	L	2.2–2.7	2.3–2.6	2.72–2.89	2.44	2.5
	W	2.1	2–2.3	2.2–2.4	2.44	2.3
m3	L	2.9	2.6–2.8	3.16–3.49	2.81	3.2
	W	2.2	2–2.2	2.29–2.53	2.19	2.5

hypolophid is present. The m3 of V16506 has a small mesoconid on the short ectolophid, and an incipient ectomesolophid.

COMPARISONS

The new specimens from the AS-5 horizon differ from cocomyids and tamquammyids in having a submolariform p4 with a distinct hypoconulid, and a talonid that is wider than the trigonid. The new species shares with *Advenimus ulungurensis* the following features: lower cheek teeth increase in size distally, metaconids of molars are situated anterior to protoconids, short hypolophid on m1 leads to anterior side of base of hypoconulid, and molars have weak postprotocristids and ectolophids. Compared to the holotype of *A. ulungurensis*, one specimen reported here (V16499) has a smaller m3 and weaker hypolophid and ectolophid of m3, whereas the other specimen (V16506) differs from the holotype of *A. ulungurensis* in having a mesoconid and an ectomesolophid on m3.

Advenimus includes three species: *A. burkei* (type species) (Dawson, 1964), *A. hupeiensis* (Dawson et al., 1984), and *A. ulungurensis* (Meng et al., 2001). *A. burkei* and *A. hupeiensis* are represented only by lower jaws and dentitions. *A. ulungurensis* differs from *A. hupeiensis* in having less bulbous cusps on cheek teeth, a metaconid more anteriorly extended, a postprotocristid weaker, and a hypoconid-hypoconulid connection stronger. *A. ulungurensis* differs from *A. burkei* in having p4 talonid wider than trigonid, a metaconid leaning more anteriorly, a hypolophid less developed and extended to the anterior base of the hypoconulid, and a talonid basin more open.

Advenimus hupeiensis Dawson et al., 1984

HOLOTYPE: IVPP V5248, right mandible with p4–m3 (Dawson et al., 1984).

REFERRED SPECIMEN: A left mandible with m1–m3 (V16507).

LOCALITY AND HORIZON: The holotype is from early Eocene Yuhuangding Formation of Dajian, Hubei. The referred specimen is from the NM-3 in the Wulanboerhe section of the Huheboerhe-Nuhet-ingboerhe area, Erlian Basin, Nei Mongol, which is considered earliest Eocene (fig. 2).

EMENDED DIAGNOSIS: Medium-sized ctenodactyloid; the masseteric crest extending anteriorly to a level between m2 and m3; the preprotocristid and postprotocristid of m1–2 well-developed; the mesoconid of lower molars distinct; the ectolophid complete; and the hypolophid short. Differs from *A. burkei* in

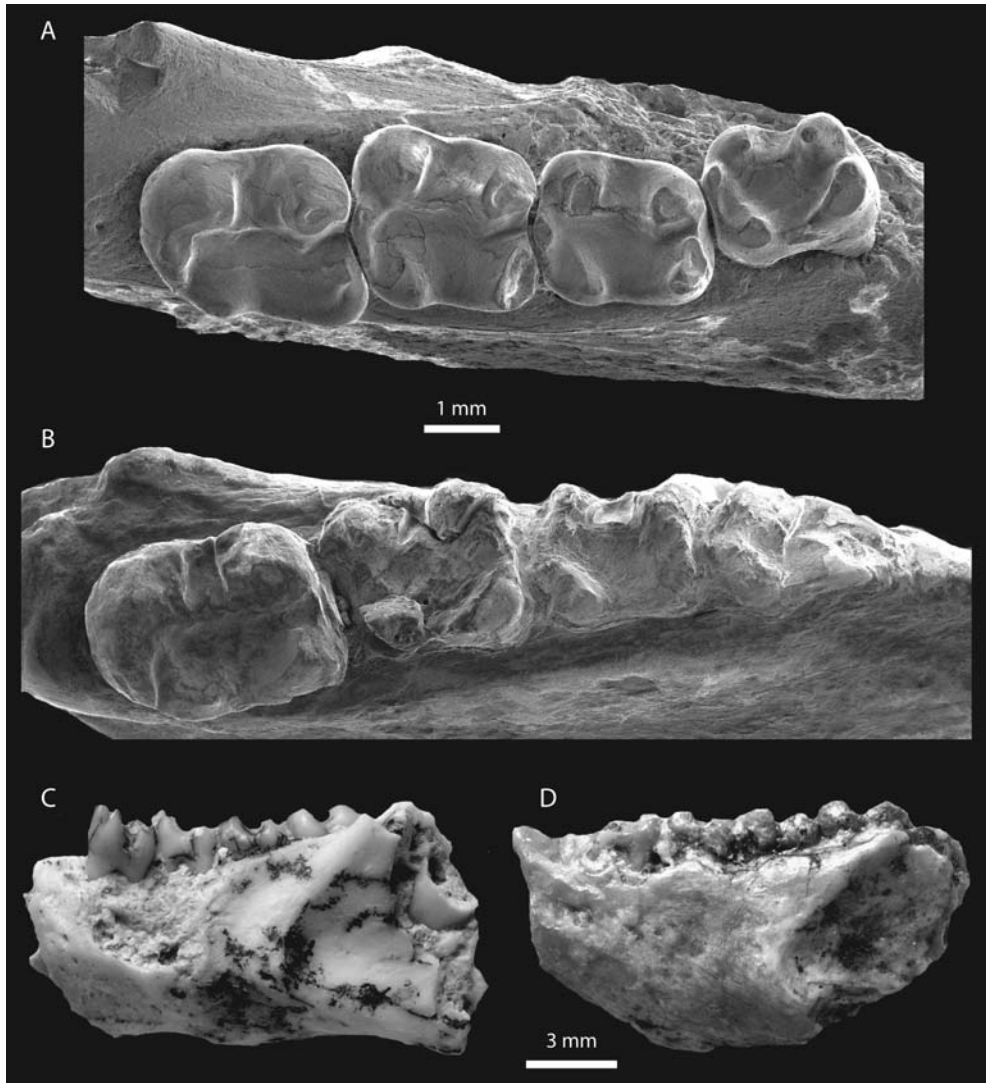


FIG. 15. Mandibles of *Advenimus ulungurensis* in occlusal view. **A**, V16499, a left mandible fragment with p4–m3; **B**, V16506, a left mandible fragment with p4–m3; **C**, V16499, labial view; **D**, V16506, labial view. A–B and C–D each to common scale.

having a shorter, free hypolophid, and a longer postprotocristid. Differs from *A. ulungurensis* in having a longer postprotocristid, a more distinct mesoconid, and a weak connection between the hypoconid and hypoconulid.

DESCRIPTION

This new incomplete jaw shows a distinct masseteric fossa that extends forward to a level between m2 and m3 (fig. 16B). The fossa is shallow and broad, and is bounded by distinct crests above and below.

Tooth measurements (length/width in mm) are: m1 (2.40/1.90), m2 (2.50/2.20), m3 (3.00/2.30). The lower molars increase in size from anterior to posterior (fig. 16A). The metaconid of m1 is broken, and

TABLE 7. Measurements of lower teeth of *Chenomys orientalis* (mm).

		V17805.1	V17805.2	V17805.3	V17805.4	Mean
p4	L	—	—	—	2.7	2.7
	W	—	—	—	2	2
m1	L	2.7	—	—	—	2.7
	W	2.4	—	—	—	2.4
m2	L	3	3	—	—	3
	W	2.7	2.8	—	—	2.75
m3	L	4	3.6	3.8	—	3.8
	W	2.6	2.8	2.8	—	2.73

the protoconid is conical. The hypoconid is the highest cusp of the talonid, and the hypoconulid is enlarged and isolated from the hypoconid and entoconid. The hypolophid of m1 is short, failing to contact either the hypoconulid or hypoconid. The ectolophid has a rounded mesoconid.

The protoconid and hypoconid of m2 are lower than the metaconid and entoconid, respectively. The metaconid is anterior to the protoconid. The preprotocristid and postprotocristid extend from the protoconid to the anterior and posterior sides of the metaconid, respectively. The trigonid is closed and short anteroposteriorly. The hypolophid is longer than that of m1, but is free. A short crest extends labially from the hypoconid and curves posteriorly toward the hypoconulid. A mesoconid is present.

The hypoconulid of m3 is weak. The crenulations of the posterior wall are distinct. The postprotocristid of m3 is shorter than that of m2. A mesoconid and minute mesostylid are present.

COMPARISONS

The new specimen from the Wulanboerhe section possesses several early ctenodactyloid rodent features, including the posterior increase in size of cheek teeth, a distinct mesoconid on the complete but relatively low ectolophid, and a large hypoconulid that is crested both labially and lingually on m1–2. Among early ctenodactyloid rodents, the short and free hypolophid is similar to those of *Stelomys*, *Xueshimys*, *Sharomys*, *Boromys*, *Saykanomys*, and *Advenimus hupeiensis*.

The new species shares the following features with *Advenimus hupeiensis*: metaconids of m2 and m3 situated anterior to protoconids, well-developed preprotocristid and postprotocristid on m2, closed trigonid on m2, short postprotocristid on m3, complete ectolophid, distinct mesoconid, and short hypolophid on lower molars. Compared with the holotype of *A. hupeiensis*, the body of the mandible of the specimen reported here is more slender than that of the holotype, and the teeth is slight more robust.

Stelomys and *Xueshimys* (Tong, 1997) are significantly smaller than the new specimen. In these two genera mesoconids are absent and the ectolophids of the lower molars are incomplete, terminating posterior to the posterior wall of the trigonid. In the new specimen, the complete ectolophid bears a rounded mesoconid and the postprotocristid is longer than that of *Xueshimys*. Moreover, the hypolophid of m2–3 of *Stelomys*, although free, is longer than that in the new specimen.

The new specimen differs from *Boromys* (Dashzeveg, 1990b) in being smaller and in having rectangular occlusal surfaces, a distinct mesoconid and a short hypolophid on m1–2. The postprotocristid of each lower molar is weaker in *Sharomys* than in the new specimen.

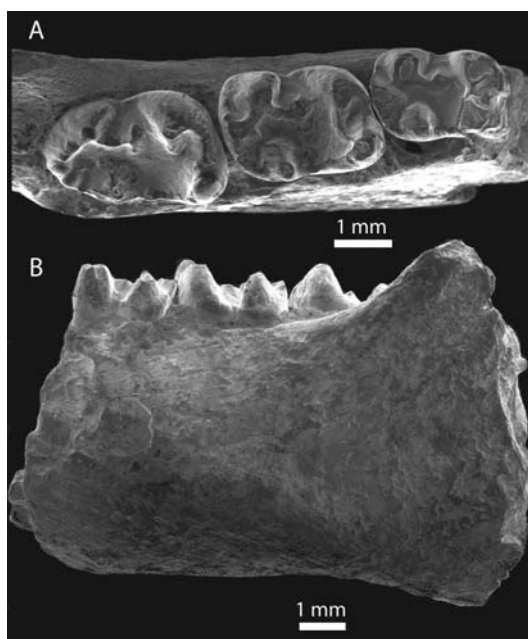


FIG. 16. A left mandible fragment with m1-3 of *Advenimus hupeiensis* (V16507). **A**, occlusal view; **B**, labial view.

Chenomys, new genus

TYPE SPECIES: *Chenomys orientalis*, sp. nov.

DIAGNOSIS: A primitive ctenodactyloid. Differs from previously known early ctenodactyloids in having a small and transverse hypoconulid on p4, metaconids and entoconids on the molars that are anterior to the protoconids and hypoconids respectively, a well-developed postprotocristid on m2, a hypolophid on m1 and m2 that extends posterolabially toward the hypoconulid, and a transverse hypolophid on m3 that contacts the ectolophid.

ETYMOLOGY: From Chinese *chen*, meaning “early, morning.”

Chenomys orientalis, new species

HOLOTYPE: A right mandible with m1–3 (V17805.1).

REFERRED SPECIMENS: V17805.2, right mandible with m2–3; V17805.3, right mandible with m3; V17805.4, right mandible with p4.

LOCALITY AND HORIZON: Huheboerhe section, Erlian Basin, Nei Mongol; NM-3, earliest Eocene (fig. 2).

DIAGNOSIS: Same as for the genus.

ETYMOLOGY: From Latin *orientalis*, “eastern, oriental.”

DESCRIPTION

A few fragmentary mandibles of this new species are preserved (fig. 17C–H; table 7). The mandible is of sciurognathous form as those of all known ctenodactyloids. The body of the mandible is robust and

deep. The angular process lies in roughly the same plane as the incisor. The deepest portion of the ramus occurs below m1 (7–7.5 mm). The masseteric fossa extends anteriorly to the level of the anterior edge of m3. The fossa is shallow and broad, lacking a distinct upper crest. There are two mental foramina: one small, below p4, and the other big, anteroventral to p4.

The trigonid basin of p4 bears a high metaconid and a small cuspsate protoconid (fig. 17A, 17C, 17E). The protoconid is connected to the metaconid by a weak postprotocristid, and the trigonid is very short anteroposteriorly. The p4 talonid is only slightly wider transversely than the trigonid and is defined by a low hypoconid, a larger entoconid, and a transverse hypoconulid. These three talonid cusps are joined along the posterior edge of the tooth. The p4 ectolophid is weak and low, and no mesoconid is present.

The lower molars are bunodont, and increase in size distally (fig. 17B). In m1 the trigonid basin is broken. The metaconid is the highest cusp on m2, and is situated anterior to the protoconid. The preprotocristid and postprotocristid of m2 are distinct, and the trigonid basin is closed. The talonid is slightly lower than the trigonid. In m1 and m2 the hypoconid is larger than the entoconid and the hypoconulid is well developed. The m1 and m2 each have a short hypolophid that extends from the entoconid posterolabially toward the hypoconulid. A distinct mesoconid is present on the complete ectolophid, but is lower than the protoconid and hypoconid. The postcingulum is low but distinct. The m3 is broader anteriorly (across the protoconid-metaconid) than posteriorly (across the entoconid-hypoconid). The m3 is morphologically similar to m2 except that the m3 postprotocristid is shorter and the m3 hypolophid is transverse and contacts the ectolophid (fig. 17B, 17F), or may extend posterolabially (fig. 17D).

COMPARISONS

Chenomys orientalis possesses several primitive ctenodactyloid features, including the lower jaw of sciurognathous form, the lower cheek teeth increasing in size distally and bunodont, the lower molar with a complete preprotocristid, and the presence of distinct mesoconids and hypoconulids on the molars. However, it differs from previously known early ctenodactyloids in having small and transverse hypoconulid on p4, hypolophid on m1 and m2 extending posterolabially toward hypoconulid, transverse hypolophid on m3 contacting ectolophid, and more posterior position of the masseteric fossa.

Primitive rodents such as *Cocomys* (Li et al., 1989) and *Exmus* (Wible et al., 2005) differ from *Chenomys* in having more conical cusps but less well-developed crests between the cusps of the molars, and in lacking a hypoconulid on p4. The primitive rodent *Bandaomys* (Tong and Dawson, 1995) is similar to *Chenomys* in having a distinct hypoconulid on p4, but differs from *Chenomys* in being smaller and in that the molars have weaker ectolophids and lack hypolophids.

Most tamquammyids differ from *Chenomys* in lacking a p4 hypoconulid, but the tamquammyids *Sharomys* and *Tsagamys* both have a small hypoconulid on p4. A distinct hypolophid is present on each lower molar of *Chenomys*, but hypolophids are absent in *Sharomys* and *Tsagamys*.

The usual absence of a p4 hypoconulid is not the only morphological feature that distinguishes tamquammyids from *Chenomys*. The following features of *Tamquammys* distinguish it from *Chenomys*: hypolophid on m1 extending to hypoconulid, transverse hypolophid contacting the ectolophid on m2 and m3, and metaconid and protoconid at same anteroposterior level. However, the hypolophids of *Chuankueimys* (Tong, 1997), *Tsinlingomys* (Li, 1963), and *Adolomys* (Shevyreva, 1989) are similar to that of *Chenomys*. *Chenomys* differs from these genera in being larger and in having more distinct mesoconids, metaconids that are more anteriorly located relative to the protoconids, and a better-developed postprotocristid on m2.

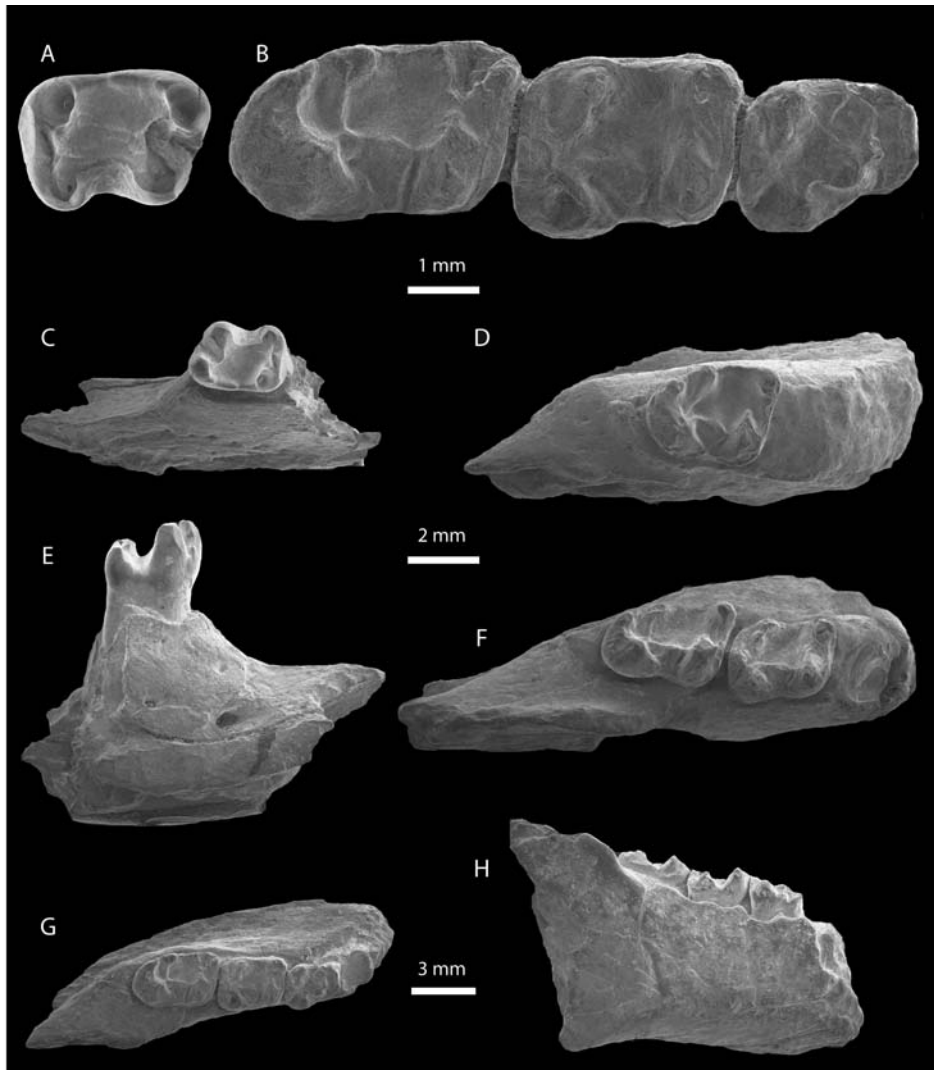


FIG. 17. Mandibles and teeth of *Chenomys orientalis*. **A**, V17805.4, right p4; **B**, V17805.1, right m1-3; **C**, V17805.4, occlusal view of a right mandible with p4; **D**, V17805.3, occlusal view of a right mandible with m3; **E**, V17805.4, labial view of a right mandible with p4; **F**, V17805.2, occlusal view of a right mandible with m2-3; **G**, V17805.1, occlusal view of a right mandible with m1-3; **H**, V17805.1, labial view. A-B, C-F, and G-H each to common scale.

Tsagankhushumys, *Bumbanomys* (Shevyreva, 1989), and *Ulanomys* (Dashzeveg, 1990a) from the Bumban Member of the Naran-Bulak Formation from Mongolia and *Juniperimus* (Shevyreva, 1996) from the Zaisan Depression of eastern Kazakhstan, lack hypolophids on their molars.

In most yuomyids and chapattimyids p4 is usually molariform and has a more distinct hypoconulid than in *Chenomys*. The p4 teeth of the yuomyids *Stelmomys* (Tong, 1997) and *Hohomys* (Hu, 1995) are similar to that of *Chenomys*, but *Chenomys* is larger than *Stelmomys* and *Hohomys*. In *Chenomys* and

Hohomys, the hypolophid on m1–2 contacts the hypoconulid, whereas the hypolophid of each lower molar of *Stelomys* is shorter and more transverse. In *Chenomys* the metaconid on m1–3 is more anteriorly positioned and the postprotocristid is better developed than in *Stelomys* and *Hohomys*.

The hypolophid of *Yuomys* is more complete than that of *Chenomys* and contacts the ectolophid at a point anterior to the hypoconid, and the mesoconid is absent. The hypolophid differs between *Advenimus* and *Chenomys*. Compared to the condition in *Chenomys*, this structure is shorter and free in *A. hupeiensis*, more transverse in *A. burkei*, and weaker and extended to the base of the hypoconulid in *A. ulungurensis*. The ectolophid, mesoconid, and postprotocristid are weaker in *A. ulungurensis* than in *Chenomys*.

Boromys and *Xueshimys* (Tong, 1997) are smaller than *Chenomys*. They differ from *Chenomys* in having such features as a protoconid of each lower molar that is parallel and opposite to the metaconid, and a free, less well-developed hypolophid. *Xueshimys* also lacks a mesoconid.

Petrokozlovia and *Saykanomys* were described by Shevyreva (1972). *Petrokozlovia* differs from *Chenomys* in that the trigonid of p4 is significantly narrower than the talonid, in having a distinct p4 hypolophid, and in lacking mesoconids on the complete ectolophids of the lower molars. *Saykanomys* differs from *Chenomys* in having a transverse hypolophid on m1–3. *Khodzhenia* (Averianov, 1996) from the uppermost Lower Eocene locality Andarak 2 in Kyrgyzstan differs from *Chenomys* in having a less well-developed postprotocristid on m2, an incomplete ectolophid, and a transverse and free hypolophid on m1–2.

Chapattimys and *Birbalomys* are from Pakistan and northwestern India (Sahni and Khare, 1973; Hussain et al., 1978). The following features of *Chapattimys* and *Birbalomys* distinguish these taxa from *Chenomys*: distinct hypolophid on p4, and molars with transverse hypolophids that contact the ectolophids. *Chapattimys* also lacks a mesoconid, and *Birbalomys* has a short or weak postprotocristid and curving ectolophid.

PHYLOGENETIC ANALYSIS

Ctenodactyloid rodents were an important component in Asian Eocene faunas. About 40 genera identified as Eocene ctenodactyloids were reported in central and eastern Asia. Recent phylogenetic analyses of ctenodactyloids show diverse results in regard to their relationships (Averianov, 1996; Wang, 1994, 1997; Dashzeveg and Meng, 1998; Marivaux et al., 2004; Wible et al., 2005) and the phylogenetic relationships of some typical Eocene ctenodactyloids, including *Yuanomys*, *Xueshimys*, *Zodiomys*, *Zoyphiomys*, *Anadianomys*, and *Hannanomys*, are still poorly known. With the new information from this study, we provide a phylogenetic analysis with focus on early ctenodactyloids. However, we realize that our analysis confronts several difficulties, including poorly documented morphologies of named species in some previous studies and our inability to gain access to the type specimens of these species. In addition, many taxa used in the analysis were based on fragmentary material or isolated teeth, which restrained the scope of the analysis. A more thorough study of the phylogenetic and taxonomic relationships of Eocene ctenodactyloids in Asia needs greater commitment and effort than we can possibly provide in this short examination. Ideally, such a study may be accomplished by an international collaboration that can incorporate all described material known to date.

TAXA AND CHARACTERS: Our analysis is based on a newly developed data matrix with 81 characters and 38 taxa at the generic level, including two eurymylids, three alagomyids and 33 ctenodactyloid

rodents. Because it has been widely accepted that basal gliroid mammals, such as eurymylids and mimotomids, share a common ancestor with rodents and lagomorphs (Li, 1977; Li et al., 1987; Meng and Wyss, 2001; Meng et al., 2003), we therefore selected two Late Paleocene eurymylids, *Heomys* (Li, 1977) and *Hanomys* (Huang et al., 2004), as outgroup taxa and used them to root the optimal trees generated by our analysis. Most ctenodactyloid genera from the Bumban Member, Tsagan Khushu, Mongolia, were not included in our phylogenetic analysis because we did not have access to the original specimens and the published material is not very clear, as we noted above. Of the 81 characters, 74 are dental, 3 cranial, and 4 mandibular. Among these characters, 21 were used previously by Marivaux et al. (2004), Wible et al. (2005), Meng and Wyss (2001), Wang (2001a), and Dashzeveg and Meng (1998); 31 characters are modified from previous work, and 29 characters are new. The character list is given in appendix 1 and the data matrix is given in appendix 2. Most of the scorings were based on direct observations of specimens and casts, but several taxa were scored based on the literature.

RESULTS: The TNT (tree analysis using new technology) phylogenetic analysis program (Goloboff et al., 2008) was used to search for the most parsimonious trees, with the Traditional Search Method. Tree visualization and character mapping were performed in PAUP v4.0B10 (Swofford, 2002). Six equally most parsimonious trees were obtained. Each tree has the tree length of 458 steps, a consistency index (CI) of 0.352 and a retention index (RI) of 0.564.

The strict consensus tree is illustrated in figure 18. Our phylogenetic analysis suggests that: *Chenomys* and *Simplicimys* are basal ctenodactyloids, *Chuankueimys* is the sister of *Tsinlingomys*, and the two together constitute the sister clade of *Yongshengomys*. Our analysis supports Wang's phylogeny in that the Ctenodactylidae is monophyletic (Wang, 1994, 1997, 2001a; Dashzeveg and Meng, 1998), which appears in our analysis as a monophyletic clade including *Protataromys*, *Tataromys*, *Karakoromys*, *Sayimys*, *Distylomys*, and *Ctenodactylus* (fig. 18). This clade is diagnosed by 11 synapomorphies: precingulum on P4 weak or absent (CI = 0.4), P3 absent (CI = 1), anterocone of each upper molar absent (CI = 0.5), precingulum of each upper molar contacting the protocone (CI = 0.5), sinus between protocone and hypocone transverse and shallow or deep (CI = 0.3), mesosinus on M1–2 U-shaped (CI = 0.5), hypoconulid of each lower molar possessing large anteriorly extended crescent (CI = 0.429), hypoconulid on m3 larger than that of m2 (CI = 0.25), hypoconid on each lower molar joined to the hypoconulid (CI = 0.25), cheek teeth with distinct lophs and weak cusps (CI = 0.429) and large mental foramen positioned below p4 (CI = 0.5).

Wang's (2001b) analysis showed that *Gobiomys*, *Mergenomys*, *Youngomys*, and Ctenodactyloidea indet. from Kazakhstan may belong to one family, known as the Gobiomyidae. In our analysis *Gobiomys* and *Mergenomys* are sister taxa, forming a monophyletic clade. The synapomorphic features supporting this sister pairing include: precingulum on DP4 short (CI = 0.667), mesostyle on each upper molar weak (CI = 0.222), metaloph on each upper molar absent (CI = 0.3), hypocone positioned lingually at same level as protocone on M2 (CI = 0.222), metaconid on p4 larger than protoconid (CI = 0.333), trigonid on m2 narrower than talonid (CI = 0.182), inner postcingulum between hypoconulid and entoconid absent (CI = 0.222), and sinusid on m1–3 deep and transverse (CI = 0.5).

Our phylogenetic analysis also suggests that *Chapattimys*, *Birbalomys*, *Dianomys*, *Petrokozlovia*, and *Yuomys* form a monophyletic clade (fig. 18), which we refer to as the *Yuomys* clade. The clade is supported by the following synapomorphies: parastyle on P4 absent (CI = 0.286), precingulum on P4 dis-

tinct (CI = 0.4), metaconid on p4 positioned opposite to the protoconid (CI = 0.167), hypolophid present on p4 (CI = 0.333), posterior zygomatic root at or posterior to level of M1 (CI = 0.333), cheek teeth with distinct lophs and weak cusps (CI = 0.429), and one mental foramen present (CI = 0.5).

DISCUSSION

TAXONOMY IN THE CTENODACTYLOIDEA

Simpson (1945) included no extinct taxa within Ctenodactyloidea, although in his classification three extinct Oligocene and/or Miocene genera, *Tataromys*, *Karakoromys*, and *Sayimys* were included in ?Anomaluroidea and ?Thryonomyidae, and these taxa were later shown convincingly to be ctenodactylids by Bohlin (1946). The family Ctenodactylidae was used by Wood (1977) to include the Asian Eocene genera *Saykanomys*, *Advenimus*, *Tsinlingomys*, and *Yuomys*, distributed in China, Mongolia, and Kazakhstan. Shevyreva (1983) reported Eocene ctenodactylids from the Nemegt Basin of Mongolia and proposed that Tamquammyidae include *Adlomys*, *Tsagankhushumys*, *Geitonomys*, *Advenimus*, *Woodomys*, *Bumbanomys*, and *Tamquammys*. Dawson et al. (1984) established two ctenodactylid families, Cocomyidae and Yuomyidae, based on absence or presence of molariform P4 and p4 in those ctenodactylids.

Several earliest ctenodactylid rodents were reported from the Bumban Member of the Naran-Bulak Formation at the Tsagan Khushu locality in the Nemegt Basin, Mongolia, by Shevyreva (1989) and Dashzeveg (1990a). These taxa have since caused considerable taxonomic confusions, as pointed out in several studies (Tong and Dawson, 1995; Averianov, 1996; Meng and Li, 2010). In addition to pointing out the taxonomic problems of the Bumbanian rodents, Averianov (1996) recognized two families, Chapattimyidae and Tamquammyidae, among ctenodactylids, and considered Yuomyidae (Dawson et al., 1984) to be a junior synonym of Chapattimyidae Hussain et al., 1978, and Cocomyidae (Dawson et al., 1984; Li et al., 1989; Dashzeveg, 1990a) and Oromomyidae (Dashzeveg, 1990b) as junior synonyms of Tamquammyidae Shevyreva, 1983. Tong (1997) divided Eocene ctenodactylids into five families: Cocomyidae, Tamquammyidae, Tataromyidae, Yuomyidae, and Chapattimyidae, whereas Dashzeveg and Meng (1998) considered several families, including Tamquammyidae, Cocomyidae, Yuomyidae, and Chapattimyidae, to be paraphyletic. There have been considerably diverse opinions on what taxa should be referred to Ctenodactyloidea and how many families Ctenodactyloidea contain.

In our phylogenetic analysis only Alagomyidae, Gobiomyidae, Ctenodactylidae, and *Yuomys* clade are recognized to be monophyletic. Some family- or subfamily-level taxa traditionally recognized, such as Cocomyidae and Yuomyidae (Dawson, 1984), Cocomyinae and Advenimurinae (Dashzeveg, 1990a), Tamquammyidae and Chapattimyidae (Averianov, 1996), and Tamquammyidae and Yuomyidae (Tong, 1997), are not monophyletic in our analysis (fig. 18). This result supports the view that several ctenodactylid families are paraphyletic (Dashzeveg and Meng, 1998; Averianov, 1996; Wang, 2001a). However, again, owing to the poor preservation of some early ctenodactylid rodents, the complicated history of taxonomic studies on the group and the unavailability of some important, particularly the holotype, specimens, we have found it to be extremely difficult to conduct a thorough phylogenetic analysis for ctenodactylids. This is also partly reflected by the low CI in our phylogenetic analyses, which probably results from missing data and the mosaic distributions of character states. Thus, even for those groups

that were recognized as monophyletic, we would view the results with caution. After a great effort to examine the Eocene ctenodactyloids of Asia, we realized that sorting out the confusion accumulated over the last few decades is beyond the scope of this report. Dashzeveg and Meng (1998) suggested that these family names of the ctenodactyloids should be used with caution, or simply the use of Ctenodactyloidea without reference to a specific family for the Eocene genera. It appears that this is perhaps the best way at this time to treat taxonomic positions for many indisputable ctenodactyloids that cannot be confidently placed in any family.

STEM TAXA OF CTENODACTYLOIDEA

Meng and Li (2010) described *Yuanomys* from the Bumbanian *Gomphos* bed in Erlian Basin and suggested that *Yuanomys* displayed several primitive dental features and were more similar to alagomyids than to cocomyids and paramyids in some aspects. As discussed by Meng et al. (2007a), the primary difference between the tooth patterns of alagomyids and rodents of modern aspect that gave the tooth a square outline in occlusal view is the narrowing of the cheek teeth. *Yuanomys* has quadrate molars, cusped cheek teeth with distinct cusps and conules, and conical protocone and paracone on P4. These dental features show that *Yuanomys* shares some characters with early ctenodactyloids and should be included in rodents. In our phylogenetic analysis (fig. 18) *Yuanomys* is placed at the basal position of the ctenodactyloid clade.

Dawson et al. (1984) described *Cocomys* and recognized it as a member of the ctenodactyloid lineage, which extended the ctenodactyloid record into the early Eocene. McKenna and Bell (1997) placed *Cocomys* in the family Chapattimyidae in a new suborder Sciuiravida, as the most recent common ancestor of Ivanantoniidae, Sciuiravidae, Chapattimyidae, Cylindrodontidae, Ctenodactylidae, and all its descendants. Wible et al. (2005) indicated that placing *Cocomys* within Chapattimyidae is not justified in any phylogenetic analysis and suggested that the concept of Sciuiravida should be discarded because it was unsupported by the evidence at hand. In our analysis *Cocomys* is another stem taxon of the ctenodactyloid clade. *Cocomys* and typical Chapattimyidae, such as *Chapattimys* or *Birbalomys*, are not closely related genetically. In general, our analyses agree with the conclusion on the phylogenetic position of *Cocomys* in Wible et al (2005).

Cocomys (Dawson et al., 1984; Li et al., 1989) and *Exmus* (Wible et al., 2005) share with ctenodactylids many cranial features from the skull roof, orbit, mesocranium, and ear region that do not occur in North American paramyids. In their phylogenetic analysis (Wible et al., 2005) *Cocomys* and *Exmus* are sister taxa. Our analysis does not support this view, but indicates that *Cocomys* and *Exmus* are both stem taxa of the ctenodactyloid clade, with *Exmus* being more derived than *Cocomys*.

Bandaomys was originally described as a possible yuomyid by Tong and Dawson (1995), and then was moved to Tamquammyidae by Tong and Wang (2006) because its P4 and p4 are less molariform than typical yuomyids. Wible et al. (2005) did not consider *Bandaomys* to be a ctenodactyloid, and they argued that *Bandaomys* does not exhibit the basic ctenodactyloid features of cheek teeth, that is, the dentition increases in size distally and has well-developed hypoconulid on the lower molars, especially on m3. With the measurements of *Bandaomys* (V10689) we found that its cheek teeth do increase in size distally, but it may not be so distinctive compared with other ctenodactyloids. The hypoconulid on m1–2 of *Bandaomys* is smaller than that of *Cocomys*, but it is still distinct. The m3 hypoconulid of most

of the ctenodactylids is less developed than that on m1–2, so a small hypoconulid on m3 of *Bandaomys* is not unusual among ctenodactylids. Therefore, we consider *Bandaomys* to be a ctenodactylid; it is more derived than *Cocomys* in our phylogenetic analysis, which is similar to the analysis by Dashzeveg and Meng (1998) and others (Guo et al., 2000; Wang, 2001a).

MOLARIFORM OR NONMOLARIFORM P4/p4

In previous taxonomy of ctenodactylids, P4/p4 morphology, either molariform or nonmolariform, has been frequently emphasized as an important character (Dawson et al., 1984; Shevyreva, 1989; Dashzeveg, 1990a; Tong, 1997). Wang (2001a) suggested, however, that the difference between these character states was not so clear. It seems that ctenodactylid evolution may have involved a complex, homoplastic, and mosaic pattern of shifts between molariform and nonmolariform P4/p4 morphologies. Tong and Wang (2006) indicated that P4/p4 is highly variable in ctenodactylids. Some tamquammyids, such as *Tamquammys dispinorum*, *Sharomys singularis*, and *Kharomys*, have weakly developed metacones and hypocones on P4 or small hypoconulids on p4. *Bandaomys* (Tong and Dawson, 1995) has a small metacone on P4 and a tiny hypoconulid on p4. *Hohomys* (Hu, 1995) is included in Yuomyidae because it has a small hypoconulid on p4. All these features are ultimately related to the degree of molarization of P4/p4, a character whose taxonomic significance may not be as straightforward as previously believed.

Our phylogenetic analysis suggests that the *Yuomys* clade includes *Chapattimys*, *Birbalomys*, *Dianomys*, *Petrokozlovia*, and *Yuomys* and forms a monophyletic clade (fig. 18) in which P4/p4 are molariform. This suggests that the presence or absence of a molariform P4/p4 may indeed be used as a basis for classification. However, what is a molariform P4 or p4 has not been clear and consistently used. Based on the specimens we examined, we suggest that a molariform P4 or p4 should include the following characters: The paracone on P4 is similar to the metacone in size and isolated from metacone and the precingulum on P4 is distinct although the parastyle may be weak. In addition to presence of the trigonid, the talonid of the p4 has a well-developed hypoconulid and the hypolophid on p4 is distinct and transverse.

YUOMYIDAE AND CHAPATTIMYIDAE

Yuomyidae was established by Dawson et al. (1984), which includes *Advenimus*, *Saykanomys*, *Yuomys*, and *Petrokozlovia*. *Chapattimys*, *Saykanomys*, and *Petrokozlovia*, however, were included in the Chapattimyidae by Hussain et al. (1978). Wang (1994) considered Yuomyidae as a group that was composed of *Advenimus* (and *Saykanomys*), *Yuomys*, *Dianomys*, and *Petrokozlovia*, whereas Chapattimyidae include *Chapattimys*, *Birbalomys*, *Bolosomys*, *Chkhikvadzomys*, and perhaps *Boromys*. Averianov (1996) recognized two families, Chapattimyidae and Tamquammyidae, among ctenodactylids and suggested Yuomyidae (Dawson et al., 1984; Flynn et al., 1986) is a junior synonym of Chapattimyidae Hussain et al., 1978. Subsequently, Tong (1997) rearranged his Chapattimyidae and Yuomyidae. Meng et al. (2001) pointed out that Averianov's Chapattimyidae is roughly equivalent to Tong's Yuomyidae and Chapattimyidae (1996).

The relationship of the Yuomyidae and Chapattimyidae in the Ctenodactyloidea is problematic. The distinction between the Chapattimyidae and Yuomyidae has been ambiguous since their establishment (Hussain et al., 1978; Dawson et al., 1984). The similarities between Yuomyidae and Chapattimyidae were also recognized by Wang (1994). Hertenberger (1982) and Dawson et al. (1984) considered Chapattimyidae

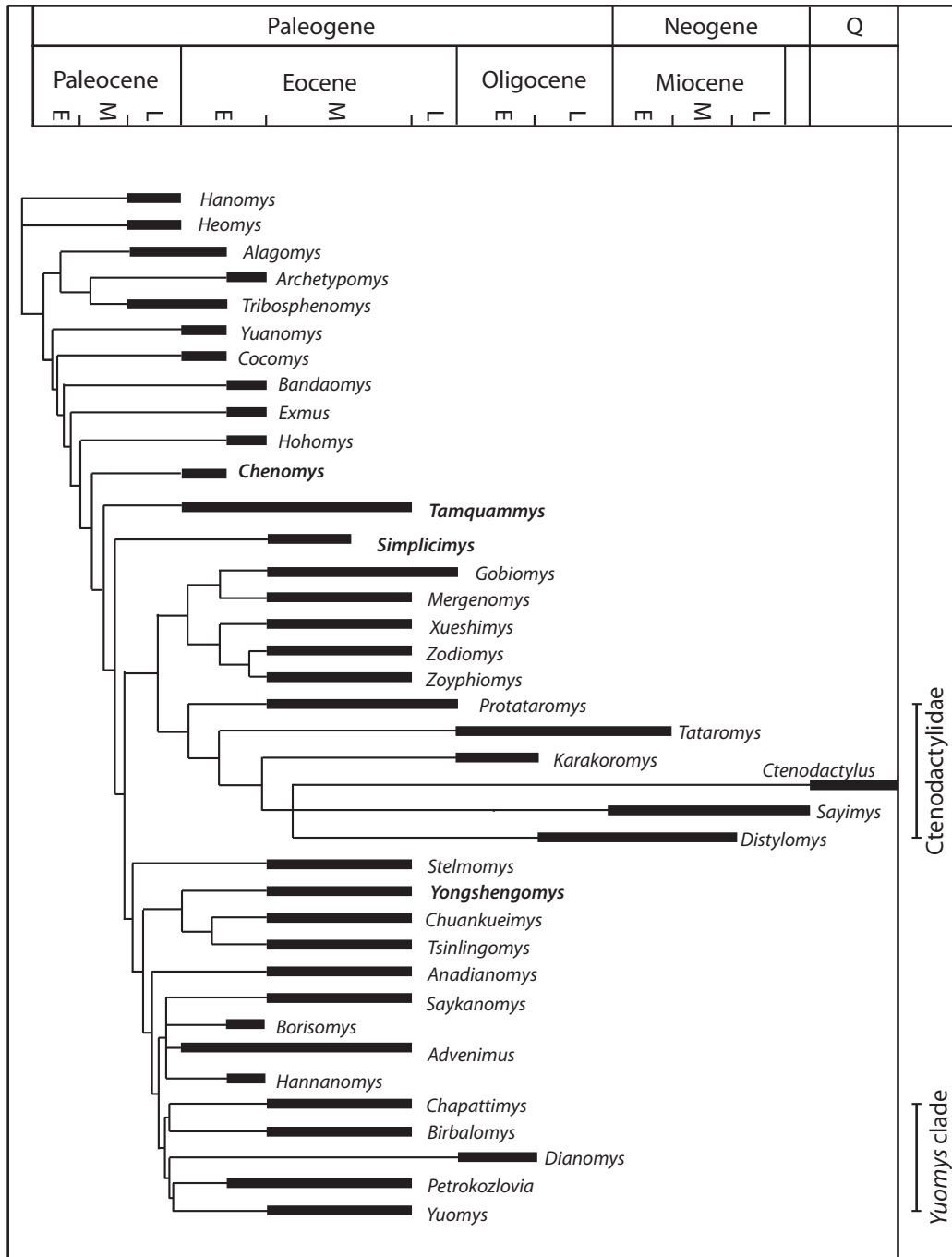


FIG. 18. Strict consensus of six most parsimonious trees generated in a phylogenetic analysis of ctenodactyloid interrelationships. See text for discussion.

to be an offshoot of primitive ctenodactyloids distributed in the Indo-Pakistan subcontinent, and Flynn et al. (1986) suggested the family is related to Miocene baluchimyines of the same realm. However, when their diagnoses are compared, the two families are distinguished from each other primarily by their molariform P4/p4 morphologies. Other features are partly overlapping, such as the hystricomorph, in both families. Our phylogenetic analysis further indicates that Dawson's (1984) Yuomyidae, Averianov's (1996) Chapattimyidae, and Tong's (1997) Yuomyidae and Chapattimyidae are not monophyletic (fig. 18). The paraphyletic nature of each family has been demonstrated by phylogenetic analyses of selected ctenodactyloids (Averianov, 1996; Dashzeveg and Meng, 1998). The monophyletic *Yuomys* clade in our analysis includes different genera from the Yuomyidae and Chapattimyidae. However, we consider that it is difficult to distinguish Yuomyidae from Chapattimyidae based only on tooth morphology. Therefore, we did not redefined Yuomyidae and Chapattimyidae, but used *Yuomys* clade temporarily for the taxa in the clade.

CONCLUSIONS

Abundant fossil ctenodactyloid rodents are found from at least six horizons from the upper part of the Nomogen Formation to the lower part of the Irdin Manha Formation in the Huheboerhe-Nuhetingboerhe area of the Erlian Basin, Nei Mongol. The materials are described and referred to 10 species that belong to six genera plus three morphotypes of Ctenodactyloidea. Described as new genera and species are *Chenomys orientalis*, *Simplicimys bellus*, and *Yongshengomys extensus*. Newly erected species are *Tamquammys robustus*, *T. longus*, and *T. fractus*, and *Yuomys huheboerhensis*.

Our phylogenetic analysis shows that several Early Eocene ctenodactyloids are paraphyletic, of which *Chenomys*, *Tamquammys*, and *Simplicimys* are placed at the base of the clade that contains the extant *Ctenodactylus*. *Yongshengomys* is the only taxon that is deeply placed within the clade containing extant *Ctenodactylus* and clustered with *Chuankueimys* and *Tsinlingomys*. Our analysis indicates that some families and subfamilies, such as Cocomyinae, Advenimurinae, Tamquammyidae, Yuomyidae, and Chapattimyidae, are probably paraphyletic.

Yuanomys, *Chenomys*, and *Tamquammys* collected from the Huheboerhe-Nuhetingboerhe area are from the upper part of the Nomogen Formation, which are the lowest strata to produce rodents with modern aspects. These genera are among the most basal ctenodactyloid rodents in our phylogenetic analyses. A recent magnetostratigraphic study places the upper part of the Nomogen Formation near the Paleocene-Eocene boundary, within the long C24r. The discovery of *Cocomys*, *Bandaomys*, *Exmus*, *Hohomys*, and *Hannanomys* in lower Eocene strata demonstrates that ctenodactyloids probably began to diversify during the early Eocene. *Tamquammys wilsoni*, *T. fractus*, *Simplicimys*, *Yongshengomys*, *Yuomys huheboerhensis*, *Yuomys* sp. A, *Yuomys* sp. B, and *Yuomys* sp. C are found from the lower part of the Irdin Manha Formation, which suggests ctenodactyloids are already highly diversified in Middle Eocene.

ACKNOWLEDGMENTS

We thank Chuankui Li, Yuanqing Wang, Zhaoqun Zhang, Yongsheng Tong, Banyue Wang, Xijun Ni, Tao Deng, and Qi Zhao for suggestions and discussions pertaining to various aspects of the research; Xun Jin, Ping Li, and Bin Bai for assistance in lab research; Yuanqing Wang, K.C. Beard, D.L. Gebo,

Xijun Ni, Wei Chen, Wei Zhou, Shejie Li, Qiang Chao, Wei Gao, Rui Yang, Chenkai Sun, Ping Li, Fangyuan Mao, and Haibin Wang for assistance in fieldwork; Yanghua Wang and Qi Li for specimen preparation; and Wending Zhang and Jie Zhang for photography. Corwin Sullivan helped to improve the manuscript and illustrations. We are grateful to Mary R. Dawson and Lawrence J. Flynn for instructive and critical comments that helped to improve the manuscript. This research was provided by China Scholarship Council, Chinese Academy of Sciences (KZCX2-EW-106), National Basic Research Program of China (973 Program) (2012CB821900), the National Natural Science Foundation of China (40802009), State Key Laboratory of Palaeobiology and Stratigraphy (Nanjing Institute of Geology and Palaeontology, CAS) (133107) and the Special Fund for Fossil Excavation and Preparation, CAS, and the China Geological Survey (nos. 1212011120115 and 1212011120142).

REFERENCES

- Asher, R.J., et al. 2005. Stem Lagomorpha and the antiquity of Glires. *Science* 307: 1091–1094.
- Averianov, A.O. 1996. Early Eocene Rodentia of Kyrgyzstan. *Bulletin du Muséum National d'Histoire Naturelle, Paris (4^e série)* 18C: 663–671.
- Bai, B., Y.-Q. Wang, and J. Meng. 2010. New craniodental materials of *Litolophus gobiensis* (Perissodactyla, “Eomoropidae”) from Inner Mongolia, China, and phylogenetic analyses of Eocene chalicotheres. *American Museum Novitates* 3688: 1–27.
- Berkey, C.P., and W. Granger. 1923. Later sediments of the desert basins of central Mongolia. *American Museum Novitates* 77: 1–16.
- Berkey, C.P., and F.K. Morris. 1924. Basin structures in Mongolia. *Bulletin of the American Museum of Natural History* 51 (5): 103–127.
- Berkey, C.P., and F.K. Morris. 1927. Geology of Mongolia: a reconnaissance report based on the investigations of the years 1922–1923. *Natural History of Central Asia*, vol. 2. New York: American Museum of Natural History.
- Bohlin, B. 1946. The fossil mammals from the Tertiary deposits of Taben-buluk, western Kansu. Part II: Simplicidentata, Carnivora, Artiodactyla, Perissodactyla, and primates. *Palaeontologia Sinica (New Series C)* 8b: 1–259.
- Bowen, G.J., P.L. Koch, J. Meng, J. Ye, and S.-Y. Ting. 2005. Age and correlation of fossiliferous Late Paleocene–Early Eocene strata of the Erlian Basin, Inner Mongolia, China. *American Museum Novitates* 3474: 1–26.
- Dashzeveg, D. 1990a. The earliest rodents (Rodentia, Ctenodactyloidea) of Central Asia. *Acta Zoologica Cracoviensia* 33: 11–35.
- Dashzeveg, D. 1990b. New trends in adaptive radiation of Early Tertiary rodents (Rodentia, Mammalia). *Acta Zoologica Cracoviensia* 33: 37–44.
- Dashzeveg, D., and J. Meng. 1998. New Eocene ctenodactyloid rodents from the eastern Gobi desert of Mongolia and a phylogenetic analysis of ctenodactyloids based on dental features. *American Museum Novitates* 3246: 1–20.
- Dawson, M.R. 1964. Late Eocene Rodents (Mammalia) from Inner Mongolia. *American Museum Novitates* 2191: 1–15.
- Dawson, M.R., C.-K. Li, and T. Qi. 1984. Eocene ctenodactyloid rodents (Mammalia) of eastern central Asia. *Carnegie Museum of Natural History Special Publication* 9: 138–150.

- Flynn, L.J., L.L. Jacobs, and I.U. Cheema. 1986. Baluchimyinae, a new ctenodactyloid rodent subfamily from the Miocene of Baluchistan. *American Museum Novitates* 2841: 1–58.
- Goloboff, P.A., J.S. Farris, and K.C. Nixon. 2008. TNT, a free program for phylogenetic analysis. *Cladistics* 24: 774–786.
- Granger, W., and C.P. Berkey. 1922. Discovery of Cretaceous and older Tertiary strata in Mongolia. *American Museum Novitates* 42: 1–7.
- Guo, J.-W., Y. Wang, and X.-A. Yang. 2000. A new early Eocene ctenodactyloid rodent (Rodentia, Mammalia) and the associated mammalian fossils from Danjiangkou, Hubei. *Vertebrata Palasiatica* 38: 303–313.
- Hartenberger, J.L. 1982. A review of the Eocene Rodents of Pakistan. *Contributions from the Museum of Paleontology of the University of Michigan* 26: 19–35.
- Hu, Y.-M. 1995. New late early Eocene ctenodactyloid rodents (Rodentia, Mammalia) from Danjiangkou, Hubei. *Vertebrata Palasiatica* 33: 24–38.
- Huang, X.-S., and J.-N. Zhang. 1990. First record of Early Tertiary mammals from southern Yunnan. *Vertebrata Palasiatica* 28: 296–303.
- Huang, X.-S., C.-K. Li, M.R. Dawson, and L.-P. Liu. 2004. *Hanomys malcolmi*, a new simplicidentate mammal from the Paleocene of central China: its relationships and stratigraphic implications. *Bulletin of Carnegie Museum of Natural History* 36: 81–89.
- Hussain, S.T., H. de Bruijn, and J.M. Leinders. 1978. Middle Eocene rodents from the Kala Chitta Range (Punjab, Pakistan) (I). *Proceedings of the Koninklijke Nederlandse Akademie van Wetenschappen (Amsterdam), series B* 81: 74–112.
- Jin, X. 2012. New mesonychid (Mammalia) material from the lower Paleogene of the Erlian Basin, Nei Mongol, China. *Vertebrata Palasiatica* 50: 245–257.
- Li, C.-K. 1963. Paramyid and sciuravids from North China. *Vertebrata Palasiatica* 7: 151–160.
- Li, C.-K. 1975. *Yuomys*, a new ischyromyoid rodent genus from the upper Eocene of north China. *Vertebrata Palasiatica* 13: 58–70.
- Li, C.-K. 1977. Paleocene eurymyloids (Anagalida, Mammalia) of Qianshan, Anhui. *Vertebrata Palasiatica* 15: 103–118.
- Li, C.-K., and S.-Y. Ting. 1983. The Paleogene mammals of China. *Bulletin of Carnegie Museum of Natural History* 21: 1–98.
- Li, C.-K., Z.-X. Qiu, D.-F. Yan, and S.-H. Xie. 1979. Notes on some Early Eocene mammalian fossils of Hengtung, Hunan. *Vertebrata Palasiatica* 17: 71–80.
- Li, C.-K., R.W. Wilson, M.R. Dawson and L. Krishtalka. 1987. The origin of rodents and lagomorphs. In H.H. Genoways (editor), *Current mammals*: 97–108. New York: Plenum.
- Li, C.-K., J.-J. Zheng, and S.-Y. Ting. 1989. The skull of *Cocomys lingchaensis*, an Early Eocene Ctenodactyloid rodent of Asia. In C.C. Black and M.R. Dawson (editors), *Papers on fossil rodents in honor of Albert Elmer Wood*. Natural History Museum of Los Angeles County Science Series 33: 179–192.
- Li, C.-K., J. Meng, and Y.-Q. Wang. 2007. *Dawsonolagus antiquus*, a primitive lagomorph from the Eocene Arshanto Formation, Nei Mongol, China. *Bulletin of Carnegie Museum of Natural History* 39: 97–110.
- Li, Q. 2012. Middle Eocene cricetids (Rodentia, Mammalia) from the Erlian Basin, Nei Mongol, China. *Vertebrata Palasiatica* 50: 237–244.
- Li, Q., and J. Meng. 2010. *Erlianomys combinatus*, a primitive myodont rodent from the Eocene Arshanto Formation, Nuhetingboerhe, Nei Mongol, China. *Vertebrata Palasiatica* 48: 133–144.

- Li, Q., and J. Meng. 2013. Eocene ischyromyids (Rodentia, Mammalia) from the Erlian Basin, Nei, Mongol, China. *Vertebrata Palasiatica* 51: 289–304.
- Mao F.-Y., and Y.-Q. Wang. 2012. Coryphodontids (Mammalia: Pantodonta) from the Erlian Basin of Nei Mongol, China, and their biostratigraphic implications. *Vertebrata Palasiatica* 50: 258–280.
- Marivaux, L., J.L. Welcomme, M. Vianey-Liaud, and J.J. Jaeger. 2002. The role of Asia in the origin and diversification of hystricognathous rodents. *Zoologica Scripta* 31: 225–239.
- Marivaux, L., M. Vianey-Liaud, and J.J. Jaeger. 2004. High-level phylogeny of early Tertiary rodents: dental evidence. *Zoological Journal of the Linnean Society* 142: 105–134.
- Matthew, W.D., and W. Granger. 1926. Two new perissodactyls from the Arshanto Eocene of Mongolia. *American Museum Novitates* 208: 1–5.
- McKenna, M.C., and S.K. Bell. 1997. Classification of mammals above the species level. New York: Columbia University Press, 631 pp.
- Meng, J. 1990. A new species of Didymoconidae and comments on related locality and stratigraphy. *Vertebrata Palasiatica* 28: 206–217.
- Meng, J., and C.-K. Li. 2010. New rodents from the Earliest Eocene of Nei Mongol, China. *Vertebrata Palasiatica* 48: 390–401.
- Meng, J., and A.R. Wyss. 2001. The morphology of *Tribosphenomys* (Rodentiaformes, Mammalia): phylogenetic implications for basal Glires. *Journal of Mammalian Evolution* 8: 1–71.
- Meng, J., W.-Y. Wu, and J. Ye. 2001. A new species of *Advenimus* (Rodentia, Mammalia) from the Eocene of northern Junggar Basin of Xinjiang, China. *Vertebrata Palasiatica* 39: 185–196.
- Meng, J., Y.-M. Hu, and C.-K. Li. 2003. The osteology of *Rhombomylus* (Mammalia, Glires): implications for phylogeny and evolution of Glires. *Bulletin of the American Museum of Natural History* 275: 1–247.
- Meng, J., et al. 2004. *Gomphos elkema* (Glires, Mammalia) from the Erlian Basin: evidence for the Early Tertiary Bumbanian Land Mammal Age in Nei-Mongol, China. *American Museum Novitates* 3425: 1–24.
- Meng, J., C.-K. Li, X.-J. Ni, Y.-Q. Wang, and K.C. Beard. 2007a. A new Eocene rodent from the lower Arshanto Formation in the Nuhetingboerhe (Camp Margetts) area, Inner Mongolia. *American Museum Novitates* 3569: 1–18.
- Meng, J., et al. 2007b. New stratigraphic data from the Erlian Basin: implications for the division, correlation, and definition of Paleogene lithological units in Nei Mongol (Inner Mongolia). *American Museum Novitates* 3570: 1–31.
- Meng, J., et al. 2007c. New material of Alagomyidae (Mammalia, Glires) from the late Paleocene Subeng locality, Inner Mongolia. *American Museum Novitates* 3597: 1–29.
- Meng, J., et al. 2009. A new species of *Gomphos* (Glires, Mammalia) from the Eocene of the Erlian Basin, Nei Mongol, China. *American Museum Novitates* 3670: 1–11.
- Ni, X.-J., K.C. Beard, J. Meng, Y.-Q. Wang, and D.L. Gebo. 2007. Discovery of the first early Cenozoic euprimate (Mammalia) from Inner Mongolia. *American Museum Novitates* 3571: 1–11.
- Ni, X.-J., et al. 2009. A new tarkadectine primate from the Eocene of Inner Mongolia, China: phylogenetic and biogeographic implications. *Proceedings of the Royal Society B* 277: 247–256.
- Qi, T. 1987. The Middle Eocene Arshanto fauna (Mammalia) of Inner Mongolia. *Annals of Carnegie Museum* 56: 1–73.
- Qiu, Z.-X., and Z.-D. Qiu. 1995. Chronological sequence and subdivisions of Chinese Neogene mammalian faunas. *Palaeogeography, Palaeoclimatology, Palaeoecology* 116: 41–70.

- Radinsky, L.B. 1964. Notes on Eocene and Oligocene fossil localities in Inner Mongolia. *American Museum Novitates* 2180: 1–11.
- Russell D.E., and R.-J. Zhai. 1987. The Palaeogene of Asia: mammals and stratigraphy. *Sciences de la Terre Series C* 52: 1–488.
- Sahni, A., and S. K. Khare, 1973. Additional Eocene mammals from the Subathu Formation of Jammu and Kashmir. *Journal of the Palaeontological Society of India* 17: 31–49.
- Shevyreva, N.S. 1971. The first find of Eocene rodents in the USSR. *Bulletin of the Georgian Academy of Science* 61: 745–747.
- Shevyreva, N.S. 1972. New Paleogene rodents from Mongolia and Kazakhstan. *Paleontological Journal (Moscow)* 3: 134–145.
- Shevyreva, N.S. 1983. New rodents of early Eocene of Postaltai Gobi (Mongolia). *In* E.M. Gromov (editor), *Rodents*: 55–58. Leningrad: Sciences Press.
- Shevyreva, N.S. 1989. New rodents (Ctenodactyloidea, Rodentia, Mammalia) from the Lower Eocene of Mongolia. *Journal of Paleontology* 3: 60–72.
- Shevyreva, N.S. 1996. New rodents (Rodentia, Mammalia) from the Lower Eocene of the Zaisan Depression (Eastern Kazakhstan). *Paleontological Journal* 30: 81–94.
- Simpson, G.G. 1945. The principles of classification and a classification of mammals. *Bulletin of the American Museum of Natural History* 85: 1–350.
- Sun, B., et al. 2009. The magnetostratigraphy of early Paleogene strata of Erlian Basin. *Journal of Stratigraphy* 33: 62–68.
- Swofford, D. L. 2002. PAUP*4.0. Phylogenetic analysis using parsimony (and other methods). Sunderland, MA: Sinauer Associates.
- Tong, Y.-S. 1997. Middle Eocene small mammals from Liguanqiao Basin of Henan Province and Yuanqu Basin of Shanxi Province, Central China. *Paleontologica Sinica (New Series C)* 26: 1–256
- Tong, Y.-S. and M.R. Dawson. 1995. Early Eocene rodents (Mammalia) from Shandong Province, People's Republic of China. *Annals of Carnegie Museum* 64: 51–63.
- Tong, Y.-S., and J.-W. Wang. 2006. Fossil mammals from the Early Eocene Wutu Formation of Shandong Province. *Paleontologica Sinica (New Series C)* 28: 1–195
- Wang, B.-Y. 1994. The Ctenodactyloidea of Asia. *In* Y. Tomida, C.-K. Li, and T. Setoguchi (editors), *Rodent and lagomorph families of Asian origins and diversification*. National Science Museum Monographs 8: 35–47.
- Wang, B.-Y. 1997. The mid-Tertiary Ctenodactylidae (Rodentia, Mammalia) of eastern and central Asia. *Bulletin of the American Museum of Natural History* 234: 1–88.
- Wang, B.-Y. 2001a. Late Eocene ctenodactylids (Rodentia, Mammalia) from Qujing, Yunnan, China. *Vertebrata Palasiatica* 39: 24–42.
- Wang, B.-Y. 2001b. Eocene ctenodactylids (Rodentia, Mammalia) from Nei Mongol, China. *Vertebrata Palasiatica* 39: 98–114.
- Wang, B.-Y., and S.-Q. Zhou. 1982. Late Eocene mammals from Pingchangguan Basin, Henan. *Vertebrata Palasiatica* 20: 203–215.
- Wang, J.-W. 1978. *Amyndon* and paramyid from Tongbo area in Henan, China. *Vertebrata Palasiatica* 16: 22–29.
- Wang, Y.-Q., J. Meng, and X. Jin. 2012. Comments on Paleogene localities and stratigraphy in the Erlian Basin, Nei Mongol, China. *Vertebrata Palasiatica* 50: 181–203.
- Wang, Y.-Q., et al. 2010. Early Paleogene stratigraphic sequences, mammalian evolution and its response to environmental changes in Erlian Basin, Inner Mongolia, China. *Science China Earth Science* 53: 1918–1926.

- Wood, A.E. 1977. The evolution of the rodent family Ctenodactylidae. *Journal of the Palaeontological Society of India* 20: 120–137.
- Wible, J.R., Y.-Q. Wang, C.-K. Li, and M.R. Dawson. 2005. Cranial anatomy and relationships of a new ctenodactyloid (Mammalia, Rodentia) from the Early Eocene of Hubei Province, China. *Annals of Carnegie Museum* 74: 91–150.
- Ye, J. 1983. Mammalian fauna from the Late Eocene of Ulan Shiren area, Inner Mongolia. *Vertebrata Palasiatica* 21: 109–118.

APPENDIX 1

CHARACTERS IN THE PHYLOGENETIC ANALYSES

We use a dental terminology (shown in figure 1) and any characters drawn from other authors' works have been modified to match our terminology.

Upper premolar

1. Size of P4: (0) $P4 < M1$, (1) $P4 = M1$, (2) $P4 > M1$. Corresponds to character 9 of Marivaux et al. (2004), but states are different.
2. Protoconule on P4: (0) absent, (1) small, (2) expanded. Corresponds to character 10 of Marivaux et al. (2004), but states are different.
3. Metaconule on P4: (0) strong, (1) weak, (2) indistinct. Corresponds to character 11 of Marivaux et al. (2004).
4. Metacone on P4: (0) strong, (1) weak, (2) absent. Corresponds to character 14 of Marivaux et al. (2004), but states are different.
5. Hypocone on P4: (0) absent, (1) weak, (2) strong. Corresponds to character 15 of Marivaux et al. (2004).
6. Parastyle on P4: (0) absent, (1) weak, (2) strong, forms an anterior lobe. New character.
7. Mesostyle on P4: (0) absent, (1) weak, (2) strong. Corresponds to character 16 of Marivaux et al. (2004).
8. Protoloph on P4: (0) complete, (1) incomplete, lingual protoloph absent, (2) absent. Corresponds to character 12 of Marivaux et al. (2004), but states are different.
9. Metaloph or postprotocrista on P4: (0) absent, (1) postprotocrista incomplete (lingual part absent), (2) postprotocrista complete, (3) metaloph complete and connecting with protocone, (4) metaloph developed but not connecting with protocone. Corresponds to character 13 of Marivaux et al. (2004), but states are different.
10. Precingulum on P4: (0) absent or weak, (1) distinct, (2) developed and distinct parastyle. New character.
11. Shape of P4 in occlusal view: (0) triangular, (1) oval, (2) rectangular. New character.
12. P3: (0) oval in crown view and multicuspate, (1) small and conical, (2) absent. Corresponds to character 8 of Wible et al. (2005).
13. Paraconule on DP4: (0) absent, (1) present. New character.
14. Precingulum on DP4: (0) short, (1) long but low, (2) long and parastyle distinct. Corresponds to character 18 of Marivaux et al. (2004), but states are different.

Upper molar

15. Hypocone: (0) small, lower than protocone, (1) distinct, (2) strong. Corresponds to character 48 of Marivaux et al. (2004), but states are different.
16. Parastyle: (0) absent, (1) small, (2) well developed, (3) forms an anterior lobe (on M1). Corresponds to character 51 of Marivaux et al. (2004).

17. Mesostyle: (0) weak, (1) strong. Corresponds to character 50 of Marivaux et al. (2004), but states are different.
18. Anterocone: (0) absent, (1) weak, (2) developed. New character.
19. Paraconule: (0) submerged in the protoloph to absent, (1) small (<1/2 of protocone), (2) large (>1/2 of protocone). Corresponds to character 62 of Marivaux et al. (2004), but states are different.
20. Metaconule: (0) strong, same with metacone, (1) reduced (<metacone), (2) absent, (3) two metaconules. Corresponds to character 55 of Marivaux et al. (2004), but states are different.
21. Precingulum: (0) absent, (1) low and isolated from the protocone, (2) connected to the protocone, (3) long and unconnected to the protocone. Corresponds to character 54 of Marivaux et al. (2004), but states are different.
22. Protoloph: (0) one, (1) two. New character.
23. Direction of protoloph: (0) long and connecting with paracone, (2) short and connecting with paraconule, (2) connecting with parastyle. New character.
24. Postparaconule crista: (0) present, (1) absent. New character.
25. Sinus between protocone and hypocone: (0) shallow, (1) distinct and extending to middle crown, (2) deep and extending to base of crown, (3) transverse and shallow or deep. New character.
26. Metaloph: (0) joining protocone, (1) toward but not joining protocone, (2) parallel to the protoloph, (3) absent. Corresponds to character 9 of Dashzeveg and Meng (1998), but states are different.
27. Entoloph: (0) absent, (1) weak, (2) distinct. Corresponds to character 66 of Marivaux et al. (2004), but states are different.
28. Centrocrista: (0) absent, (1) weak. Corresponds to character 45 of Meng and Wyss (2001), but states are different.
29. Hypocone position in relation to protocone on M2: (0) aligned with the protocone, (1) more labial than the protocone, (2) more lingual than the protocone. New character.
30. M1 length/width proportion: (0) length < width, (1) length = width, (2) length > width. New character.
31. Upper molar shape: (0) triangular, (1) rectangular. Corresponds to character 14 of Wible et al. (2005).
32. Preprotoconule: (0) absent, (1) present. New character.
33. Metacone position in relation to paracone on upper molar: (0) more lingual than the paracone, (1) aligned. New character.
34. The mesosinus on M1–2: (0) V-shaped, (1) U-shaped. New character.

Lower premolar

35. Talonid of p4: (0) narrower than trigonid, (1) slightly wider than trigonid, (2) much wider than trigonid. Corresponds to character 21 of Marivaux et al. (2004), but states are different.
36. Predominant cuspids on p4: (0) metaconid = protoconid, (1) metaconid > protoconid, (2) protoconid > metaconid. Corresponds to character 22 of Marivaux et al. (2004), but states are different.
37. Metaconid-protoconid position on p4: (0) opposed, (1) protoconid posterior. Corresponds to character 38 of Marivaux et al. (2004).
38. Anteroconid on p4: (0) absent, (1) small. New character.
39. Hypoconulid on p4: (0) absent, (1) weak, (2) strong. Corresponds to character 26 of Marivaux et al. (2004).
40. Preprotocristid on P4: (0) absent, (1) complete. Corresponds to character 29 of Marivaux et al. (2004), but states are different.
41. Postprotocristid on P4: (0) absent, (1) incomplete, unconnected to metaconid, (2) complete. Corresponds to character 30 of Marivaux et al. (2004).

42. Ectolophid on p4: (0) absent, (1) present, (2) middle position. Corresponds to character 28 of Marivaux et al. (2004), but states are different.
43. Hypolophid on p4: (0) absent, (1) present. Corresponds to character 23 of Marivaux et al. (2004).
44. Size of p4: (0) $p4 < m1$, (1) $p4 > m1$. Corresponds to character 33 of Marivaux et al. (2004), but states are different.
45. Anteroconid on dp4: (0) absent, (1) weak, (2) strong. Corresponds to character 36 of Marivaux et al. (2004).
46. Mesoconid on dp4: (0) absent, (1) distinct. Corresponds to character 45 of Marivaux et al. (2004), but states are different.
47. Preprotocristid on dp4: (0) absent, (1) incomplete, unconnected to metaconid, (2) complete. Corresponds to character 41 of Marivaux et al. (2004).
48. Postprotocristid on dp4: (0) absent, (1) complete. Corresponds to character 42 of Marivaux et al. (2004), but states are different.
49. Hypolophid of dp4: (0) absent, (1) low, interrupted labially, (2) developed and connect with hypoconid, (3) developed and connect with hypoconulid. New character.
50. Direction of ectolophid on dp4: (0) oblique, (1) straight. New character.

Lower molar

51. Anteroconid: (0) present, (1) absent. Corresponds to character 75 of Marivaux et al. (2004), but states are different.
52. Trigonid height: (0) higher than talonid, (1) same as talonid. Corresponds to character 97 of Marivaux et al. (2004).
53. Width of trigonid on m2: (0) narrower than talonid, (1) same as talonid, (2) slight wider than talonid. Corresponds to character 98 of Marivaux et al. (2004), but states are different.
54. Hypoconulid: (0) simple cuspid, (1) strong, expanded, (2) submerged into the posterolophid, (3) large crescent of anteriorly extended. Corresponds to character 92 of Marivaux et al. (2004), but states are different.
55. Hypoconulid on m3: (0) greater than that of m2, (1) subequal to that of m2, (2) reduced, submerged into the posterolophid. Corresponds to character 40 of Wible et al. (2005), but states are different.
56. Hypoconulid and entoconid: (0) unconnected, (1) connected. New character.
57. Hypoconulid and hypoconid: (0) unconnected, (1) connected. New character.
58. Mesostylid: (0) absent, (1) weak, (2) strong. Corresponds to character 76 of Marivaux et al. (2004).
59. Mesoconid: (0) small to absent, (1) simple cuspid, (2) transversally elongated. Corresponds to character 78 of Marivaux et al. (2004).
60. Ectolophid: (0) complete, reaches protoconid, (1) anteriorly incomplete, (2) absent. Corresponds to character 80 of Marivaux et al. (2004), but states are different.
61. Position of ectolophid: (0) more labial and oblique, (1) more labial and straight, (2) running on the midline of tooth, (3) more lingual. New character.
62. Postprotocristid on m1: (0) complete and connected to metaconid, (1) long but unconnected to metaconid, (2) short but connected to ectolophid. New character.
63. Postprotocristid on m2: (0) long but unconnected to metaconid, (1) short but connected to ectolophid, (2) complete and connected to metaconid. New character.
64. Postprotocristid on m3: (0) long but unconnected to metaconid, (1) short but connected to ectolophid, (2) complete and connected to metaconid. New character.

65. Hypolophid on m1: (0) absent, (1) low, interrupted labially, (2) developed and connected with hypoconid, (3) developed and connected with hypoconulid, (4) connected with ectolophid in front of hypoconid. New character.
66. Hypolophid on m2: (0) absent, (1) low, interrupted labially, (2) developed and connected with hypoconid, (3) developed and connected with hypoconulid, (4) connected with ectolophid in front of hypoconid. New character.
67. Hypolophid on m3: (0) absent, (1) low, interrupted labially, (2) developed and connect with hypoconid, (3) developed and connect with hypoconulid, (4) connected with ectolophid in front of hypoconid. New character.
68. Position of hypoconulid: (0) close to entoconid, (1) in the middle of hypoconid and entoconid, (2) close to hypoconid. New character.
69. Entoconid-hypoconulid connection by inner postcingulum: (1) absent, (2) low and weak, (3) distinct. New character.
70. Hypoconid-hypoconulid connection by external postcingulum: (1) absent, (2) low and weak, (3) distinct. New character.
71. Sinusid on m1–3: (0) shallow (narrower than mesosinusid) and symmetric, (1) deep (subequal to or deeper than the mesosinusid) and transverse, (2) deep and oblique posteriorly. Corresponds to character 23 of Wang (2001a).

Other (skull, mandible, and incisor)

72. Infraorbital foramen: (0) small, (1) large (hystricomorphous). Corresponds to character 53 of Wible et al. (2005).
73. Incisive foramina: (0) middle length, beginning closer to incisors, (1) middle length, beginning at middiastema, (2) nearly as long as diastema. Corresponds to character 50 of Wible et al. (2005), but states are different.
74. Posterior zygomatic root: (0) it levels with M1 or more posterior, (1) with P4, (2) anterior to P4. Corresponds to character 2 of Wang (2001a).
75. Anterior edge of masseteric fossa: (0) extends below m1, (1) below m2, (2) below m3, (3) below p4. Corresponds to character 47 of Wible et al. (2005), but states are different.
76. Cheek tooth size increases distally: (0) absent, (1) present. Corresponds to character 6 of Wible et al. (2005).
77. Cheek teeth: (0) with developed cusps and weak lophs, (1) with distinct cusps and lophs, (2) with distinct lophs and weak cusps, (3) tri- or bilobate. Corresponds to character 24 of Dashzeveg and Meng (1998), but states are different.
78. Incisor enamel: (0) pausiserial, (1) multiserial. Corresponds to character 26 of Dashzeveg and Meng (1998).
79. Mental foramina: (0) one, (1) two. Corresponds to character 42 of Wible et al. (2005), but states are different.
80. Large mental foramen position: (0) below p4, (1) in front of p4 but close to p4, (2) below diastema, (3) below m1. Corresponds to character 43 of Wible et al. (2005), but states are different.
81. The masseteric crest: (0) both upper and lower crests are present, (1) upper crest indistinct and lower crest distinct, (2) only one developed horizontal crest. Corresponds to character 4 of Wang (2001a).

All issues of *Novitates* and *Bulletin* are available on the web (<http://digitallibrary.amnh.org/dspace>). Order printed copies on the web from:

<http://shop.amnh.org/a701/shop-by-category/books/scientific-publications.html>

or via standard mail from:

American Museum of Natural History—Scientific Publications
Central Park West at 79th Street
New York, NY 10024

Ⓒ This paper meets the requirements of ANSI/NISO Z39.48-1992 (permanence of paper).